

Supplementary Materials for

Unprecedented Inorganic HTL-based MA-free Sn-Pb Perovskite Photovoltaics with an Efficiency over 23%

Seojun Lee^a, Jun Ryu^a, Dong-Gun Lee^a, Padmini Pandey^b, Chang-Mok Oh^c, In-Wook Hwang^c, SungWon Cho^a, Saemon Yoon^a, Jeong-Yeon Lee^a, and Dong-Won Kang^{, a, b}*

^a Department of Smart Cities, Chung-Ang University, 84 Heukseok-ro, Dongjak-gu, Seoul 06974, Republic of Korea.

^b Department of Energy Systems Engineering, Chung-Ang University, 84 Heukseok-ro, Dongjak-gu, Seoul 06974, Republic of Korea.

^c Advanced Photonics Research Institute, Gwangju Institute of Science and Technology, Gwangju, Republic of Korea

* Corresponding Author: Dong-Won Kang (kangdwn@cau.ac.kr)

Experimental section

Materials

Formamidinium iodide (FAI, Greatcell Solar), *n*-butylammonium iodide (*n*-BAI, Greatcell Solar), Cesium iodide (CsI, 99.999 %, Alfa Aesar), lead(II) iodide (PbI₂, 99.99 %, Tokyo Chemical Industry Co., Ltd.), tin(II) fluoride (SnF₂, 99 %, Sigma-Aldrich), Sn powder (99.8%, Sigma-Aldrich), iodine (I₂, 99.8%, Sigma-Aldrich), and germanium iodide (GeI₂, 99.8%, Sigma-Aldrich) were purchased and used as precursors for Sn-Pb binary perovskites. Ethane-1,2-diammonium iodide (EDAI₂, Greatcell Solar) was purchased and used as passivation of Sn-Pb perovskite film surface. Dimethylformamide (DMF, 99.5 %, Samchun Chemical) and dimethyl sulfoxide (DMSO, 99.8 %, Samchun Chemical), toluene (99.8 %, Samchun Chemical), 2-Propanol (IPA, Sigma-Aldrich), and chlorobenzene (CBZ, 99 % - GR grade, Wako) were used as solvents. Acetone (≥ 99 %, Samchun Chemical) and Isopropanol (IPA, ≥ 99.5 %, Samchun Chemical) were used as cleaning solvents for Fluorine-doped tin oxide (FTO)-coated glasses. Poly(3,4-ethylenedioxythiophene) polystyrenesulfonate (PEDOT:PSS, PVP AI 4083) was sourced from Clevios™ (Germany). Phenyl-C₆₁-butyric acid methyl ester (PC₆₁BM, 99.5 %) was sourced from Organic Semiconductor Materials (OSM, Republic of Korea) and Bathocuproin (BCP, 98 %) was purchased from Alfa Aesar. Poly(3-hexylthiophene-2,5-diyl) (P3HT, 4002-EE, Mw = ca. 60 K, RR = ~ 90 %) was purchased from Rieke Metals. Nickel nitrate hexahydrate (Ni(NO₃)₂·6H₂O), aluminum nitrate nonahydrate (Al(NO₃)₃·9H₂O) were purchased from Sigma-Aldrich.

Al-NiO_x nanocrystal (ANO NC) solution synthesis method

552.8 mg of nickel nitrate hexahydrate and 10 mg of aluminum nitrate nonahydrate was dissolved in 20 ml of deionized water. After fully dissolving them, sodium hydroxide was dropped into the solution until pH 10. The green murky solution was rinsed with deionized water by a centrifuge, and the rinsing was repeated 3 times. The rinsed solution was fully dried at 95 °C. Then, the dried green powder was annealed at 300 °C in the furnace, resulting in obtaining black powder which is aluminum doped nickel oxide. This powder was dispersed in 3:1 ratio of deionized water and IPA with a concentration of 12.5 mg/ml.

Preparation of perovskite precursor solution

1. Preparation of SnI₂ solution

SnI₂ solution was prepared from Sn + I₂ with 0.8 M concentration. First, 0.8M I₂ was dissolved in DMSO 0.2 mL and stirred for 1 hour. After the stirring, DMF 0.8 mL was added to the I₂ solution dissolved in DMSO and stirred for 10 min. Next, Sn powder of 0.8 M was added to the I₂ solution and stirred for overnight. Then, the SnI₂ solution suitable for the stoichiometric ratio of 1.6 M MA-free Sn-Pb perovskite was completely prepared.

2. Preparation of 1.6 M MA-free Sn-Pb perovskite solution

A BA_{0.02}(FA_{0.83}Cs_{0.17})_{0.98}Sn_{0.5}Pb_{0.5}I₃ precursor was prepared from *n*-BAI, FAI, CsI, PbI₂, with 1.6 M concentration (the stoichiometric ratio of *n*-BAI:FAI:CsI:PbI₂ is 0.83:0.17:0.5:0.5), excess SnF₂ of 0.08 M, Sn powder of 0.056 M, and SnI₂ solution. GeI₂ of 0.04 M is added for with GeI₂ Sn-Pb perovskite. After the preparation of *n*-BAI, FAI, CsI, PbI₂, SnF₂, Sn powder, and GeI₂, the filtered SnI₂ solution of 1.042 mL was added to the prepared bottle. The MA-free Sn-Pb perovskite solution was completely prepared after stirring for 2 hours.

Fabrication of MA-free Sn- Pb Perovskite Solar Cells (PSCs) and hole-only devices

FTO-coated glasses (Asahi) were sequentially cleaned with acetone, and IPA in the ultrasonic bath for 20 min, respectively. After cleaning, the glass substrates were dried in the dry oven at 95 °C to evaporate residual solvents. The cleaned substrates were then subjected to a UV treatment for 30 min. PEDOT:PSS was spin-coated onto the FTO substrates at 6000 rpm for 30 s in ambient conditions and annealed at 150 °C for 20 min on a hotplate as a hole transport layer (HTL) (thickness is ca. 20~30 nm). ANO NC of 50 µL was spin-coated FTO substrates at 1000 rpm for 1 s and 3000 rpm for 30s in ambient condition and annealed at 150 °C for 20 min on a hotplate as an inorganic hole transport layer (HTL) (thickness is ca. 10~20 nm). Then, the HTL-coated substrates were transferred to N₂-filled glove box. The perovskite precursor solutions with or without GeI₂ were spin-coated at 5000 rpm for total of 35 s (acceleration time: 5 s) in the N₂-filled glove box. A 300 µL of toluene was applied dropwise in the center of the substrate at 12~13 s during the spin coating. The perovskite-coated substrate was annealed at 65 °C for 1 min and sequentially annealed at 100 °C for 10 min (thickness is ca. 600 nm). For the passivation of the perovskite surface, the EDAl₂ with 0.5 mg/mL dissolved in IPA was spin-coated with a dynamic coating at 5000 rpm for 30 s and annealed at 100 °C for 5 min to remove residual solvent. For an electron transport layer, a PC₆₁BM solution with 20 mg/mL dissolved in CBZ was spin-coated onto the perovskite film at 1500 rpm for 35 s and annealed at 75 °C for 10 min. A BCP solution (0.5 mg/mL dissolved in IPA) was spin-coated at 4000 rpm for 20 s without any post-annealing treatment. The silver (Ag) top electrodes (ca. 180 nm) were thermally evaporated under a high vacuum condition ($< 2 \times 10^{-6}$ Torr) with a shadow mask (the size of each solar cell device is 4 mm²).

The hole-only devices for space-charge limited current (SCLC) were fabricated with a structure of FTO/PEDOT:PSS or ANO/perovskite/P3HT/Ag. All fabrication processes were followed

in the same manner with the PSCs except for a P3HT layer. A P3HT solution dissolved in CBZ (10 mg/mL) was spin-coated onto the perovskite film at 3000 rpm for 30s and annealed at 100 °C for 5 min.

Characterization

The optical absorption spectra were characterized using ultraviolet-visible (UV–Vis) spectroscopy (UV-2700, Shimadzu). Before scanning the perovskite samples, a baseline correction was conducted with a scan range of 300 nm – 1100 nm. The measurement conditions are 100 nm/min for the scan speed and 1 nm for the interval step size. The steady-state photoluminescence (PL) spectra were measured using a spectrofluorometer (Fluorolog3 with TCSPC, HORIBA SCIENTIFIC) with a laser excitation wavelength at 463 nm. A crystal structure of the perovskite films was evaluated by X-ray diffraction (XRD, D8-Advance, Bruker-AXS). A diffracted beam monochromator was equipped in the X-ray diffractometer (Cu K α radiation, $\lambda = 1.541 \text{ \AA}$). All the XRD data were recorded in the two-theta range from 10° to 40° with a 1° min⁻¹ scanning rate at RT. The surface morphologies and cross-sectional images were investigated by field emission scanning electron microscopy (FE-SEM; AURIGA, Carl Zeiss). The roughness of the perovskite films was observed by atomic force microscopy (AFM, NX10 Complete AFM, Park Systems). X-ray photoelectron spectroscopy (XPS) measurement was performed with a K-alpha system (Thermo Fisher Scientific) using a monochromatic Al K α irradiation (1486.6 eV). Ultraviolet photoelectron spectroscopy (UPS) measurement was performed using an XPS-Theta Probe (Thermo Fisher Scientific) with Al K α radiation (1486.6 eV). The steady-state fluorescence spectra were recorded using a Hitachi F-7000 fluorescence spectrophotometer. fs-TAS and decays were recorded using a homemade TA spectrometer combined with a femtosecond Ti:sapphire regenerative amplifier system (Hurricane, Spectra Physics). A pump pulse at 400 nm with a power density of 3 $\mu\text{J}/\text{cm}^2$ was

produced using an optical parametric amplifier (IR-OPA, Spectra Physics) and a neutral density filter, while a broadband white-light continuum probe pulse was generated by focusing a small portion of the 800 nm amplifier output into a sapphire window. TA signals in respective optical delays of pump and probe pulses were collected using an optical fiber coupled with multichannel spectrometers from Ocean Insight (Ocean FX). The contact angle measurement was conducted by pendant drop tensiometer (DSA100, KRUSS).

Device testing

All device characterizations were carried out in ambient conditions (RT and relative humidity (RH) of 25 – 30 %). Current-voltage (J-V) curves of the perovskite solar cells were measured using a solar simulator (PEC-L01, Peccell Technologies) under standard AM 1.5 illumination (power, 100 mW/cm²). The maximum power point tracking (MPPT) was measured under 100 mW/cm² illumination using LED solar simulator (Newport, LSH-7320). The light intensity was calibrated with a silicon photodiode detector (BS-500BK, BUNKOUKEIKI CO., LTD.). Each device was measured with a scan rate of 100 mV/s⁻¹ using a Keithley 2400 source meter. The external quantum efficiency (EQE) spectra were characterized using a CompactStat instrument (Ivium Technologies; Eindhoven, Netherlands) comprised of a power source (Abet Technologies 150 W xenon lamp, 13014) and a monochromator (DongWoo Optron, MonoRa500i). The system was calibrated with the same photodiode detector for the solar simulator. Space-charge limited current (SCLC) measurement was performed using a Keithley 2400 source meter. The scan range of the voltage was 0 V - 5 V and the measurement was conducted in a dark condition.

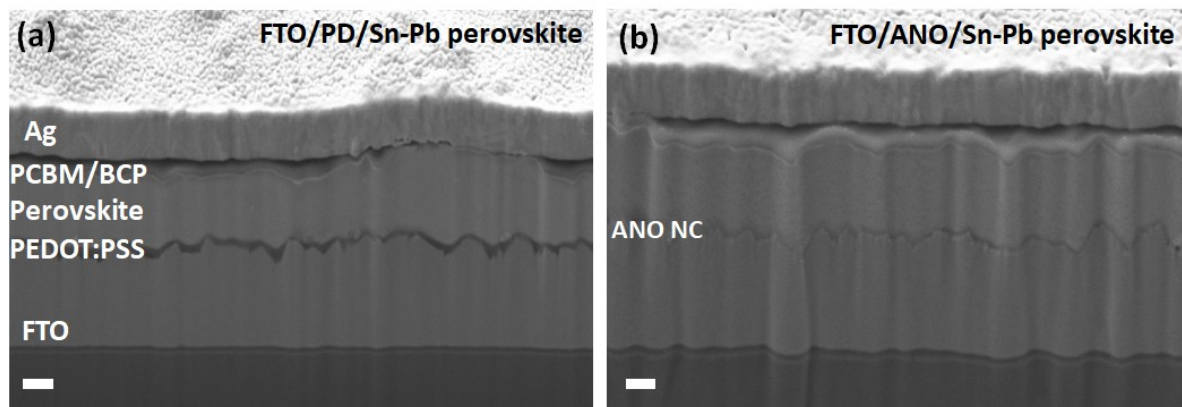


Fig. S1 The cross-sectional images for MA-free Sn-Pb perovskite devices with PEDOT:PSS (PD) and ANO NC HTLs observed by focused ion beam(FIB)-scanning electron microscope(SEM). Scale bar: 200 nm.

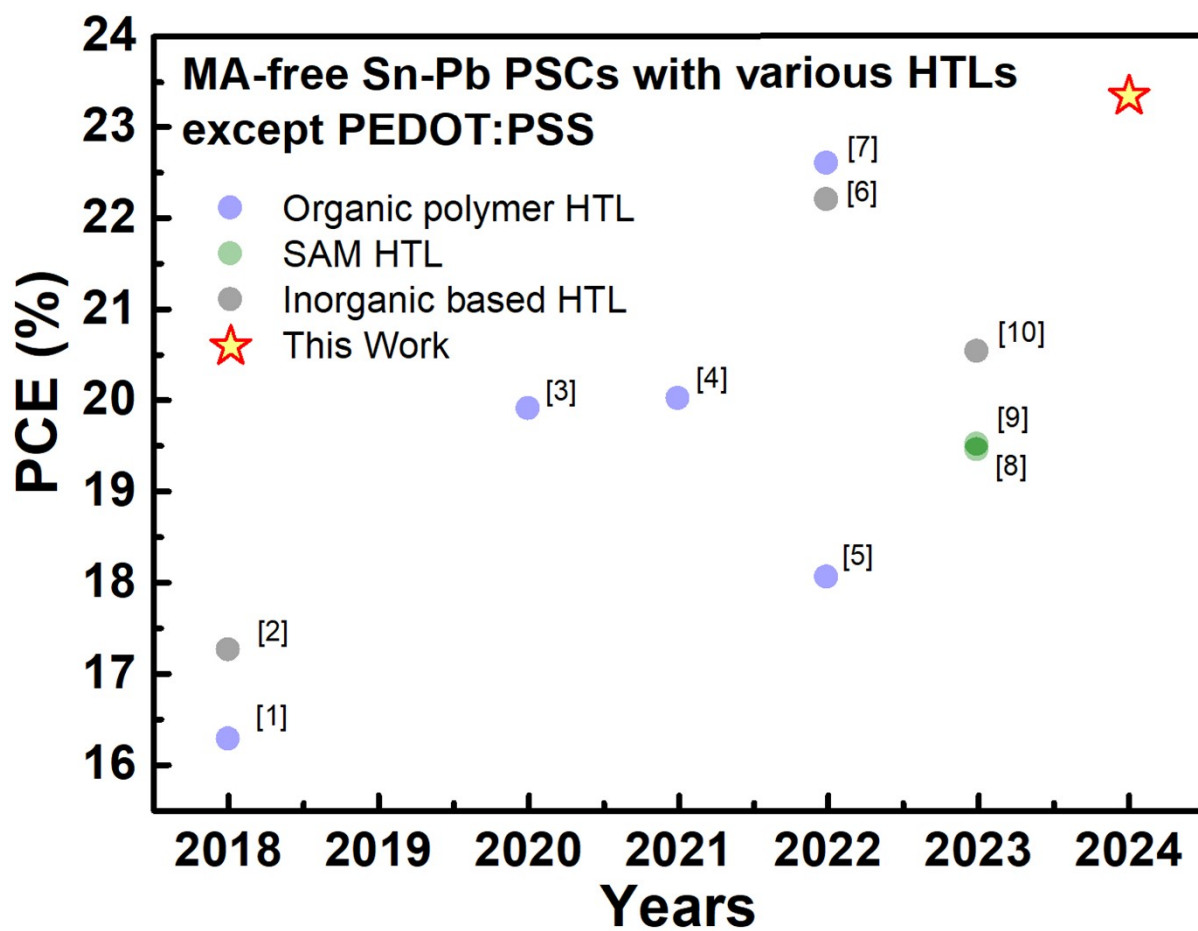


Fig. S2 PCE distribution of the MA-free Sn-Pb PSCs fabricated with various HTLs except PEDOT:PSS reported to date, including our work.¹⁻¹⁰

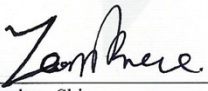
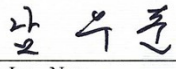


CHUNGBUK TECHNO PARK

9, Jeongtong-ro, Deoksan-myeon, Jinceon-gun, Chungbuk, Korea
TEL:+82-43-270-2472 FAX:+82-43-270-2489 <http://www.cbtp.or.kr>

CBTP-24SB-0002

TEST REPORT

Applicant	Trade Name	Chung-Ang University		
	Address	84, Heukseok-ro, Dongjak-gu, Seoul, Republic of Korea		
	Telephone Number	-	Fax Number	-
Product	Name	Perovskite Based Solar Cell		
	Model Name	Sn-Pb Perovskite Solar Cell		
	Manufacturer	Chung-Ang University		
Issued Date		2023.	11.	27.
Test Date		2023.	12.	21. ~ 2023. 12. 21.
Test Method		Refer		
Test Results		<input type="checkbox"/> Pass	<input type="checkbox"/> Fail	<input checked="" type="checkbox"/> Refer
Test Engineer		Deputy Chief Engineer		
				
Yeonbae Shin		Woo-Jun, Nam		
<p>This report only responds to the tested sample and may not be reproduced, except in full, without written approval of the CHUNGBUK TECHNO PARK. The test results presented in this report relate only to the item(s) tested.</p>				
<p>Jan. 04, 2024</p> <h3>CHUNGBUK TECHNO PARK</h3>				



CHUNGBUK TECHNOPARK

9, Jeongtong-ro, Deoksan-myeon, Jincheon-gun, Chungbuk, Korea
TEL:+82-43-270-2472 FAX:+82-43-270-2489 <http://www.cbtp.or.kr>

1. Test Laboratory






1.1 General Information

Name of Laboratory	CHUNGBUK TECHNOPARK
Representative	Roh Keun Ho
Address	40, Yeonggudanji-ro, Ochang, Cheongwon, Cheongju, Chungbuk, Korea
Telephone Number	+82-43-270-2001
Fax Number	+82-43-270-2499
Home page	www.cbtp.or.kr

1.2 Location of Test Laboratory

Address	Solar Technical Center 9, Jeongtong-ro, Deoksan-myeon, Jincheon-gun, Chungbuk-province 27872, Republic of Korea
Telephone Number	+82-43-270-2471
Fax Number	+82-43-270-2499

1.3 Accreditation Laboratory

Accreditation Items	Accordance with the provisions	Certification No.	Mark
Korea Communications Commission of Republic of Korea -Radio Equipment -Electromagnetic Interference -Electromagnetic Susceptibility	Framework Act on Telecommunications and Radio Waves Acts	KR-0115	
FCC Part 15 & 18 - EMI(Radiated & Conducted Emission)	ANSI 63.4	Registration No.924	
VCCI EMI(Radiated & Conducted Emission)	VCCI	2765	
Conformitee European EMC	2006/28/EC, ECE R10.03	ROK0820C	
Electrical Characteristics of Photovoltaic	KS C IEC 61215 : 2006 KS C 8561 : 2020 KS C IEC 60068-2-52 : 2010	KT391	

2. Test Standard

2.1 Application Certification

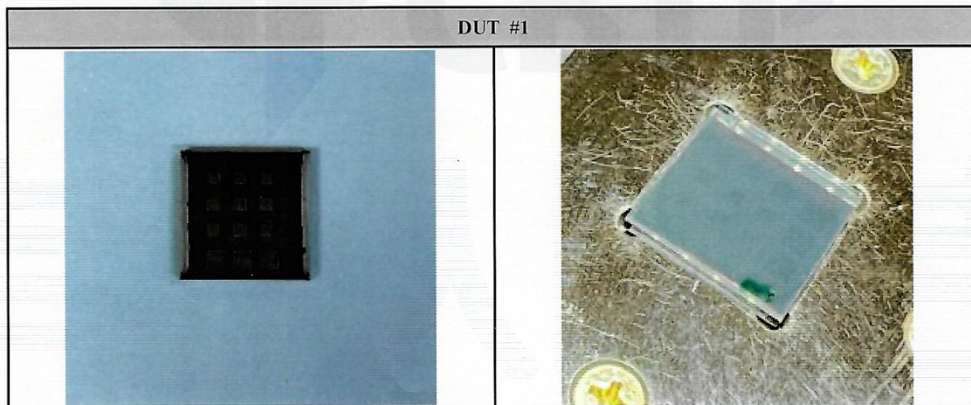
Standards	Contents
Determine the current-voltage characteristic of the module in accordance with KS C IEC 60904-1	I. Test condition a. Temperature Condition : 25 °C b. Irradiance : 100 mW/cm ² II. Apparatus a. Solar Simulator Class BBB or better in accordance with KS C IEC 60904-9

3. Information of DUT(Device Under Test)

3.1 Information of DUT

No.	Model	Structure	Area
# 1	Sn-Pb Perovskite Solar Cell	Glass/FTO/Al-NiO _x /MA-free Sn-Pb perovskite/PCBM/BCP/Ag	0.04 cm ²

3.2 Device Picture



4. Test Item and Results

4.1 Test Item

- 1) Test Purposes : Measurement of electrical and optical properties of perovskite solar cells
- 2) Laboratory environmental conditions
 - Temperature : (25 ± 1) °C
 - Humidity : (30 ± 5) % R.H.
- 3) DUT No. : # 1
- 4) Test Equipment

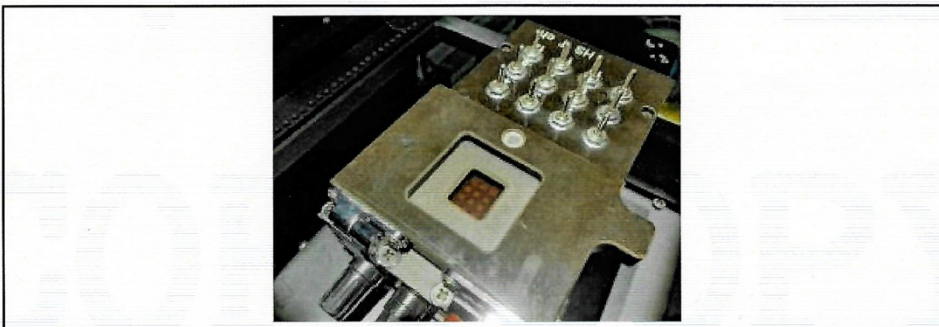
No.	Description	Model	Manufacturer
1	Cell Simulator	DKIVT-30 PV Cell IV Tester	DENKEN
2	Source meter	2401	Keithely



5) Test Methods

5.1 Measurement of Photovoltaic Current - Voltage Characteristics

- ① Set up the intensity of light and temperature of under the required conditions
- ② Calibrated using a certified cell under test conditions (AM 1.5 Global, 100 mW/cm²)
- ③ Measure and record the characteristic value (output) by connecting the electrode of the sample



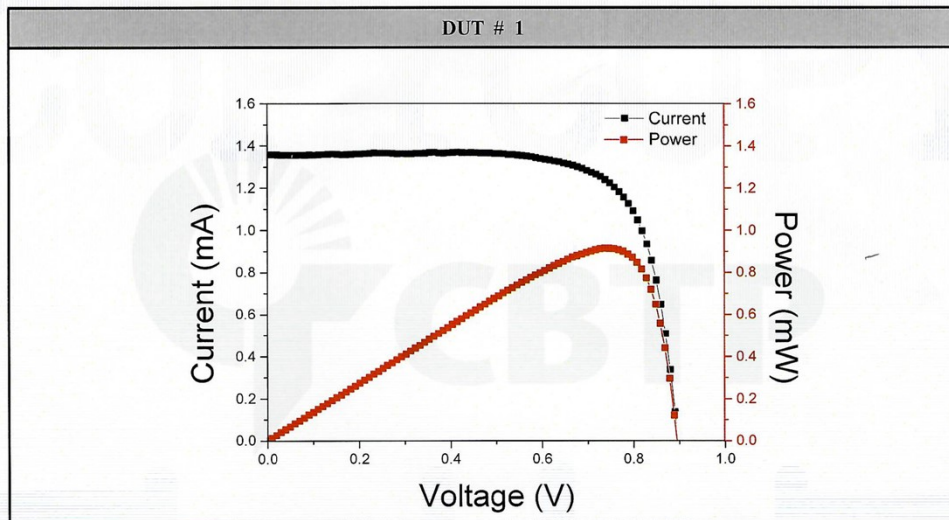
4.2 Test Results

1) Measurement of Photovoltaic Current - Voltage Characteristics

① I-V Characteristics

DUT	Voc (V)	Isc (mA)	Vmp (V)	Imp (mA)	FF (%)	Power (mW)	Efficiency (%)	Area (cm ²)
# 1	0.896	1.36	0.738	1.24	75.10	0.916	22.90	0.04

② I-V Curve



- Last page -

TEST REPORT

KIMS Korea Institute of
Materials Science
797 Changwondaero, Sungsan-gu, Changwon-si,
Gyeongsangnam-do, 51508, Korea
Tel : 055-280-3784, Fax : 055-280-3788

Report No. :
2441-0265-01359

Page 1 / 2 Pages



1. Client

- Name : Chung-Ang University Industry Academic Cooperation Foundation
- Address : (06974) 84, Heukseok-ro, Dongjak-gu, Seoul, Rep. of Korea

2. Sample Description

- Product Name : Sn-Pb binary metal halide perovskite solar cell
- Product No. : Sn-Pb_AEDL_CAU-01
- Material : Perovskite ($\text{BA}_{0.02}(\text{FA}_{0.83}\text{Cs}_{0.17})_{0.98}\text{Sn}_{0.5}\text{Pb}_{0.5}\text{I}_3$)
- No. of Item : 1 EA.

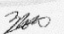
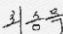
3. Date of Test : 2024. 09. 06

4. Location of Test : Permanent Testing Lab On Site Testing
(Address: 797 Changwondaero, Sungsan-gu, Changwon-si, Gyeongsangnam-do, Republic of Korea)

5. Test method used : KS C IEC 60904-8 Standard Test Method for Spectral Responsivity Measurements of Photovoltaic Devices

The QuantX-300 Quantum Efficiency Measurement System
Reference Cell: Device S/N(BD024), Device Materials(mono-Si)

6. Test Result : Refer to Test Results

Affirmation	Tested by	Approved by
	Name : Jung-Dae Kwon 	Name : Sung-Mook Choi 

The above test report is based on the test results of the test sample(s) submitted by the client.

Sept. 06, 2024.

Chul Jin Choi
Korea Institute of Materials Science

Note: 1. The results shown in this test report refer only to the sample(s) tested and KIMS do not guarantee the quality of all products of the customer.
2. This test report cannot be reproduced except in full, without the written approval of KIMS.

TEST RESULTS

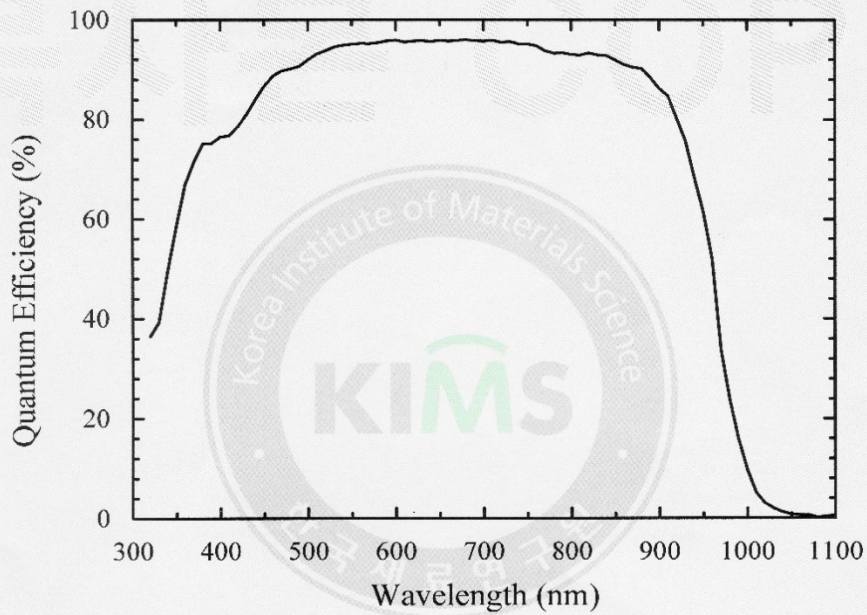
KIMS Korea Institute of
Materials Science
797 Changwondaero, Sungsan-gu, Changwon-si,
Gyeongsangnam-do, 51508, Korea
Tel : 055-280-3784, Fax : 055-280-3788

Report No. :
2441-0265-01359
Page 2 / 2 Pages



Sample: Sn-Pb_AEDL_CAU-01
Sept 06, 2024 13:56

Temperature = $25.0 \pm 2^\circ\text{C}$
Device Area = 0.04 cm^2



-Zero voltage bias

End.

Fig. S3 The certified PCE and EQE spectrum details for the champion device.

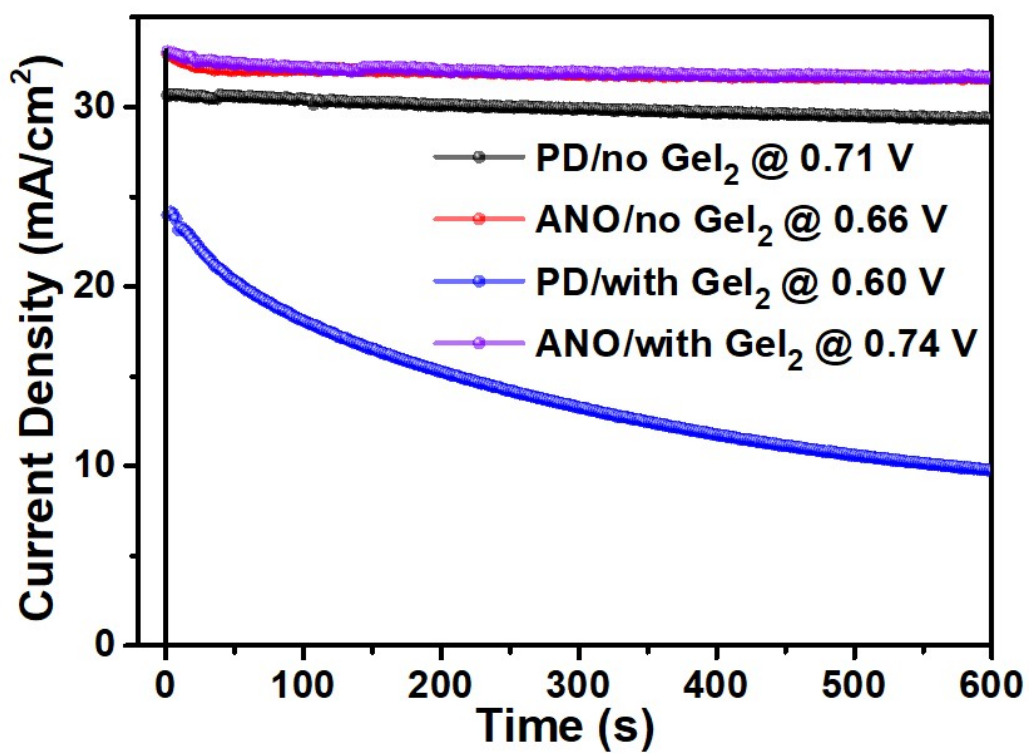


Fig. S4 Steady-state photocurrents for the perovskite solar cells with the suggested conditions for 600 s at the maximum power point.

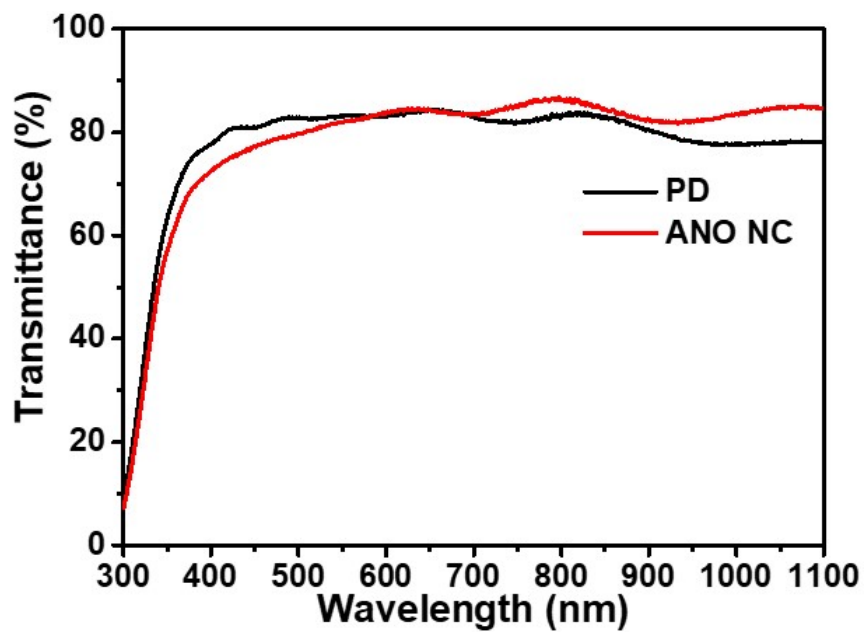


Fig. S5 Transmittance of PEDOT:PSS and ANO NC films.

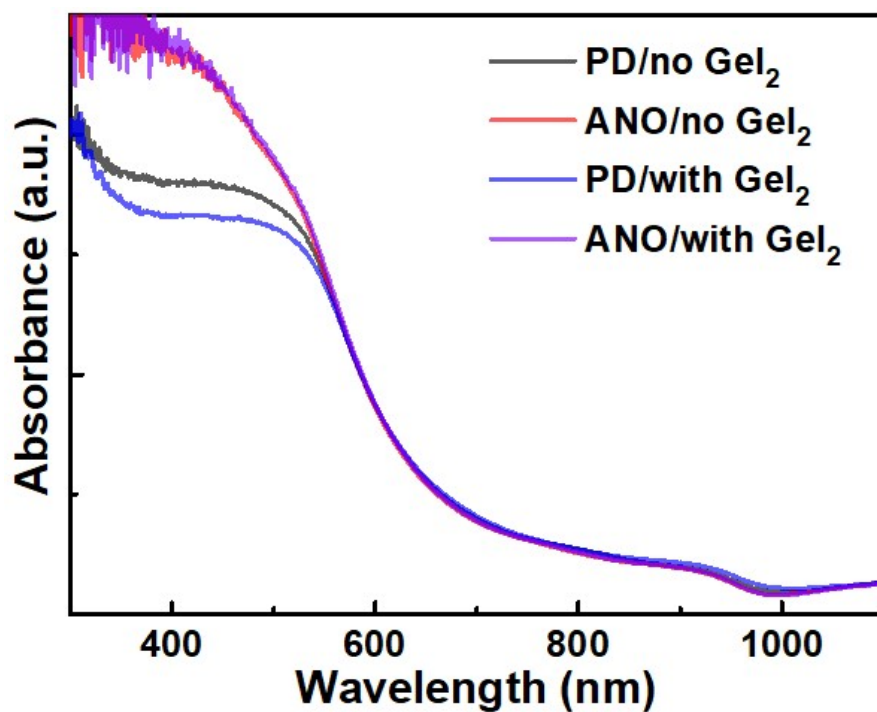


Fig. S6 Absorption spectra of the Sn-Pb perovskite films without or with GeI_2 on PEDOT:PSS or ANO HTLs.

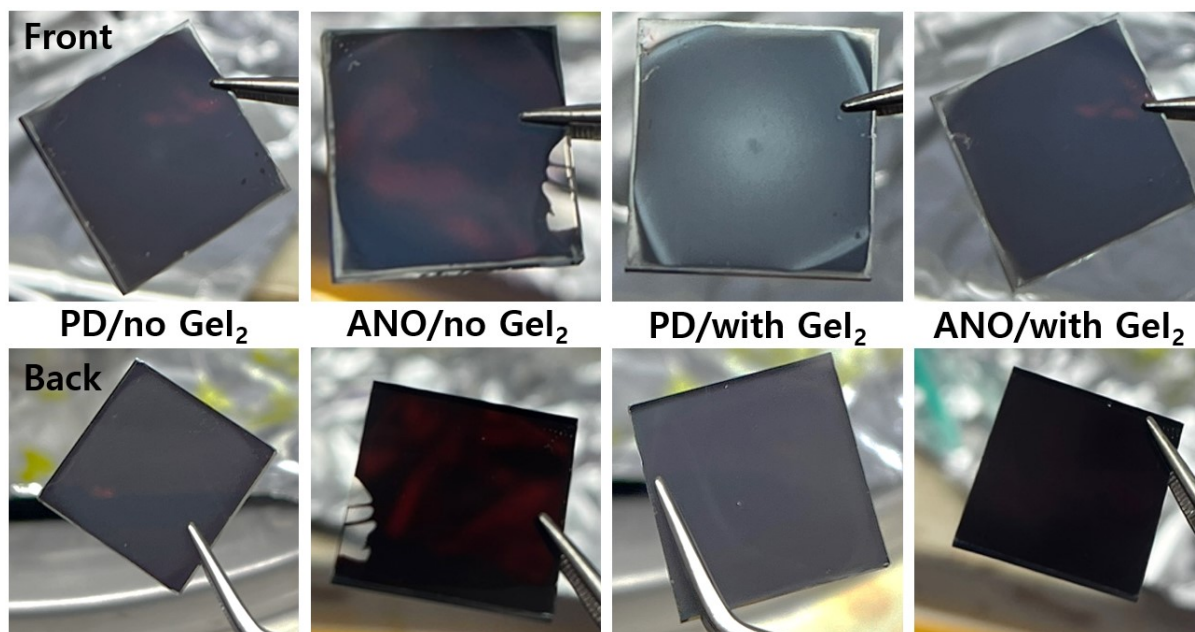


Fig. S7 Photographs of FTO/HTL/perovskite films with PD/no GeI₂, ANO/no GeI₂, PD/with GeI₂, ANO/with GeI₂ conditions.

Table S1. Photovoltaic performance parameters of the PD/no GeI₂ Sn-Pb PSCs under AM 1.5 illumination (100 mW/cm²) measured in the air (RT, RH: 30-40%)

PD/no GeI ₂ #	V _{oc} (V)	J _{sc} (mA/cm ²)	FF (%)	PCE (%)
1	0.83	31.08	67.61	17.47
2	0.85	31.29	71.82	19.04
3	0.86	31.33	73.17	19.61
4	0.86	31.35	73.72	19.84
5	0.86	31.33	74.09	19.95
6	0.86	31.26	74.34	20.04
7	0.86	31.25	74.70	20.15
8	0.85	30.78	72.36	18.85
9	0.86	31.19	74.20	19.99
10	0.86	31.63	72.12	19.57
11	0.85	31.39	74.54	19.86
12	0.85	31.40	74.57	19.93
13	0.85	31.41	74.22	19.88
14	0.82	31.36	70.20	18.05
15	0.82	30.68	70.36	17.76
16	0.83	30.68	71.15	18.05
17	0.83	30.68	70.98	18.01
18	0.82	30.64	71.20	17.91
19	0.83	31.30	74.23	19.39
20	0.84	31.19	75.78	19.89
21	0.84	31.20	74.63	19.51
22	0.84	31.15	74.28	19.35
23	0.83	31.13	73.18	18.81
24	0.83	30.01	72.59	18.12
25	0.84	30.02	73.25	18.49
26	0.84	29.93	73.40	18.45
27	0.84	29.96	73.52	18.59
28	0.84	29.85	73.55	18.51
29	0.85	29.99	73.78	18.73
30	0.85	29.89	73.95	18.71
Average	0.84±0.013	30.88±0.57	73.05±1.73	19.02±0.81

Table S2. Photovoltaic performance parameters of the ANO/no GeI₂ Sn-Pb PSCs under AM 1.5 illustration (100 mW/cm²) measured in the air (RT, RH: 30-40%)

ANO/no GeI ₂ #	V _{oc} (V)	J _{sc} (mA/cm ²)	FF (%)	PCE (%)
1	0.85	32.50	70.39	19.38
2	0.85	32.68	63.06	17.56
3	0.84	32.45	67.14	18.36
4	0.83	33.40	69.85	19.38
5	0.84	31.90	72.18	19.39
6	0.85	31.73	72.78	19.52
7	0.82	32.43	69.15	18.41
8	0.83	31.83	71.25	18.86
9	0.83	32.00	72.29	19.23
10	0.81	33.28	72.31	19.38
11	0.82	32.68	70.79	18.96
12	0.82	32.53	70.96	18.89
13	0.82	32.29	71.15	18.81
14	0.82	32.14	70.89	18.63
15	0.82	33.04	70.42	19.09
16	0.82	32.86	70.56	19.01
17	0.80	32.64	67.79	17.67
18	0.82	32.32	68.34	18.10
19	0.82	32.40	69.06	18.45
20	0.84	33.86	62.61	17.77
21	0.85	32.62	69.80	19.43
22	0.85	31.58	67.16	18.03
23	0.85	32.68	66.81	18.56
24	0.85	32.77	68.50	19.12
25	0.84	32.28	72.10	19.50
26	0.83	32.09	71.81	19.18
27	0.83	33.09	68.24	18.64
28	0.84	32.31	69.67	18.81
29	0.83	33.10	69.19	18.95
30	0.84	32.65	68.61	18.77
Average	0.83±0.014	32.54±0.51	69.50±2.46	18.79±0.55

Table S3. Photovoltaic performance parameters of the PD/with GeI₂ PSCs under AM 1.5 illumination (100 mW/cm²) measured in the air (RT, RH: 30-40%)

PD/with GeI ₂ #	V _{oc} (V)	J _{sc} (mA/cm ²)	FF (%)	PCE (%)
1	0.75	29.86	65.61	14.63
2	0.74	30.39	61.33	13.82
3	0.76	30.47	66.77	15.41
4	0.76	30.36	66.33	15.21
5	0.77	29.53	60.38	13.75
6	0.75	31.49	61.56	14.55
7	0.76	31.19	63.37	14.97
8	0.78	30.75	65.53	15.69
9	0.78	30.28	65.89	15.63
10	0.79	26.16	60.48	12.48
11	0.79	25.79	60.43	12.24
12	0.76	26.89	58.57	11.92
13	0.74	30.78	58.03	13.21
14	0.74	31.00	64.67	14.81
15	0.73	30.82	64.52	14.60
16	0.72	28.96	56.92	11.92
17	0.74	30.30	63.29	14.19
18	0.73	30.13	60.29	13.28
19	0.74	30.14	61.98	13.85
20	0.77	30.88	62.60	14.82
21	0.76	30.65	61.83	14.35
23	0.74	30.39	61.33	13.82
24	0.73	30.94	60.23	13.61
25	0.73	30.96	59.19	13.43
26	0.76	30.29	59.09	13.57
27	0.76	31.27	63.36	15.02
28	0.76	30.93	61.72	14.43
29	0.72	31.25	60.72	13.68
30	0.78	29.95	61.35	14.34
Average	0.75±0.019	30.11±1.41	61.96±2.55	14.04±1.02

Table S4. Photovoltaic performance parameters of the ANO/with GeI₂ PSCs under AM 1.5 illumination (100 mW/cm²) measured in the air (RT, RH: 30-40%)

ANO/with GeI ₂ #	V _{oc} (V)	J _{sc} (mA/cm ²)	FF (%)	PCE (%)
1	0.88	33.65	77.91	23.08
2	0.88	33.54	77.69	22.93
3	0.87	33.66	77.37	22.71
4	0.87	33.16	79.51	22.83
5	0.87	33.29	79.64	22.99
6	0.87	33.20	79.58	22.88
7	0.88	32.64	78.97	22.59
8	0.86	33.59	79.89	23.16
9	0.85	33.71	79.23	22.78
10	0.86	33.57	79.01	22.91
11	0.87	33.56	79.23	23.00
12	0.87	33.56	79.34	23.04
13	0.87	33.58	79.57	23.17
14	0.87	32.91	80.89	23.06
15	0.86	32.91	80.25	22.84
16	0.86	32.90	79.87	22.67
17	0.87	33.62	78.53	23.02
18	0.87	32.97	78.87	22.68
19	0.87	33.46	77.82	22.58
20	0.87	33.88	79.46	23.34
21	0.87	33.42	78.41	22.74
22	0.87	33.63	79.40	23.30
23	0.87	33.57	78.71	23.05
24	0.86	33.75	79.62	23.00
25	0.85	33.68	79.48	22.87
26	0.86	33.21	79.24	22.63
27	0.87	32.93	78.65	22.51
28	0.87	33.46	77.82	22.58
29	0.85	33.71	79.23	22.78
30	0.85	33.75	79.18	22.81
Average	0.87±0.007	33.41±0.32	79.08±0.79	22.88±0.22

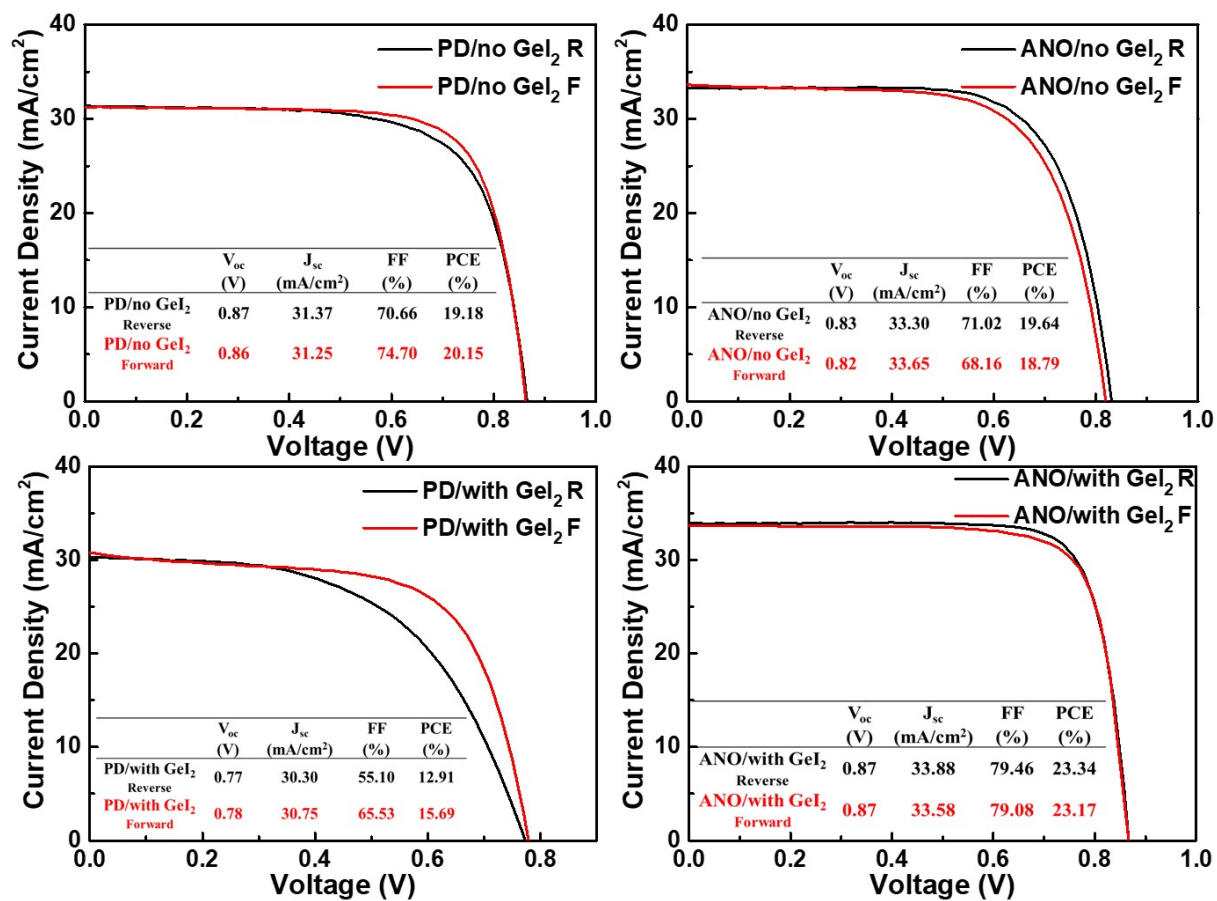


Fig. S8 J-V curves (forward and reverse scans) of the PSCs with the suggested conditions (PD/no GeI₂, ANO/no GeI₂, PD/with GeI₂, and ANO/with GeI₂)

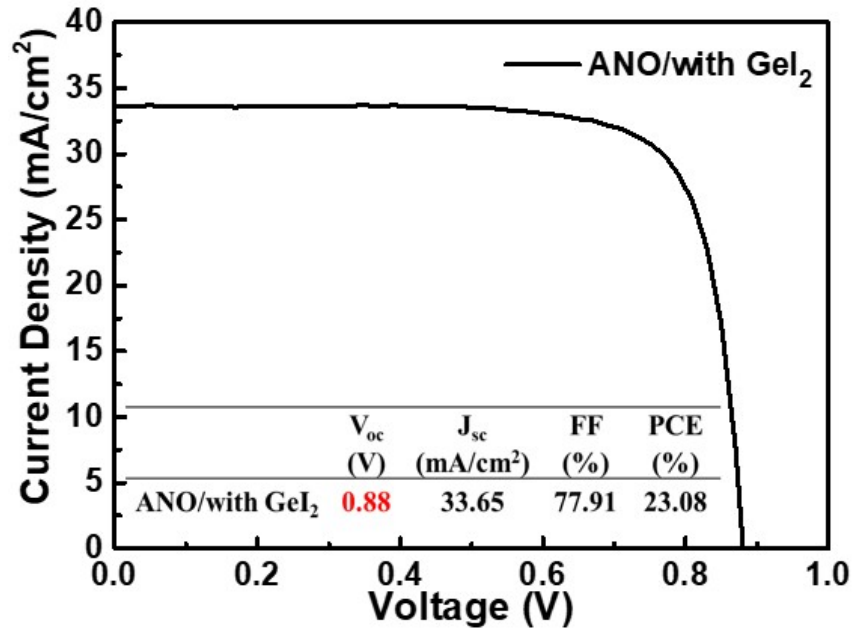


Fig. S9 J-V curve of ANO/with GeI₂ PSC with the highest V_{oc}

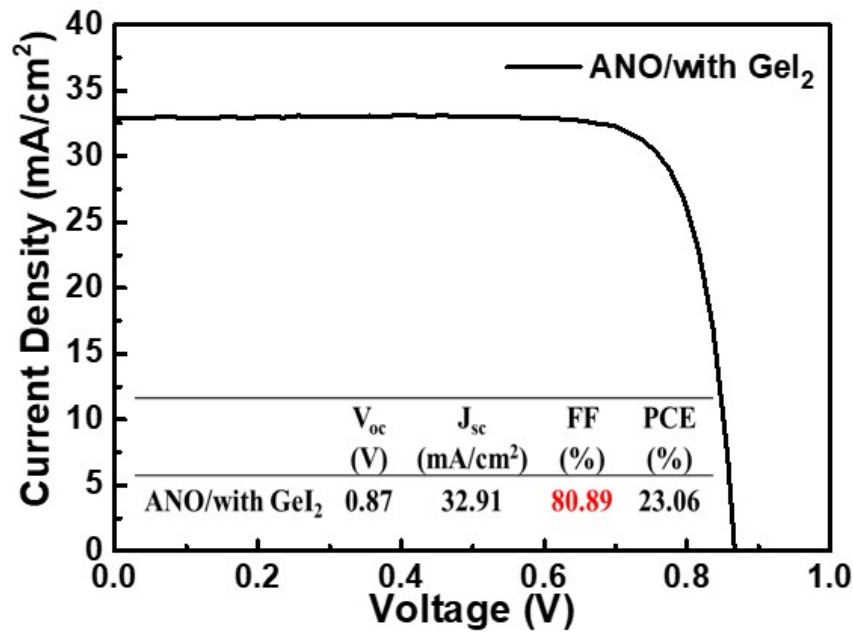


Fig. S10 J-V curve of ANO/with GeI₂ PSC with the highest fill factor

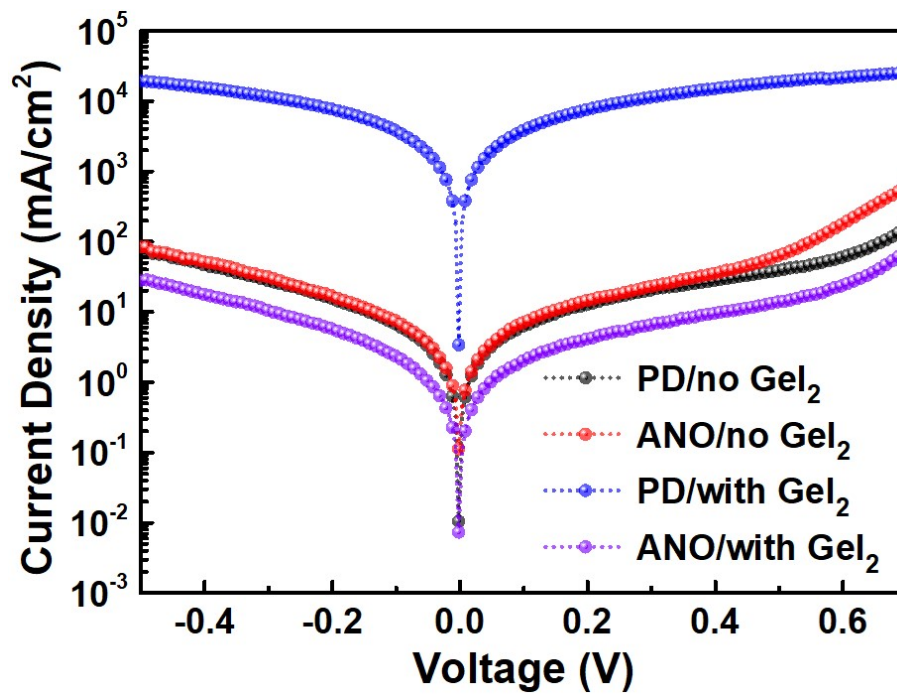


Fig. S11 The dark J-V characterization of the perovskite devices.

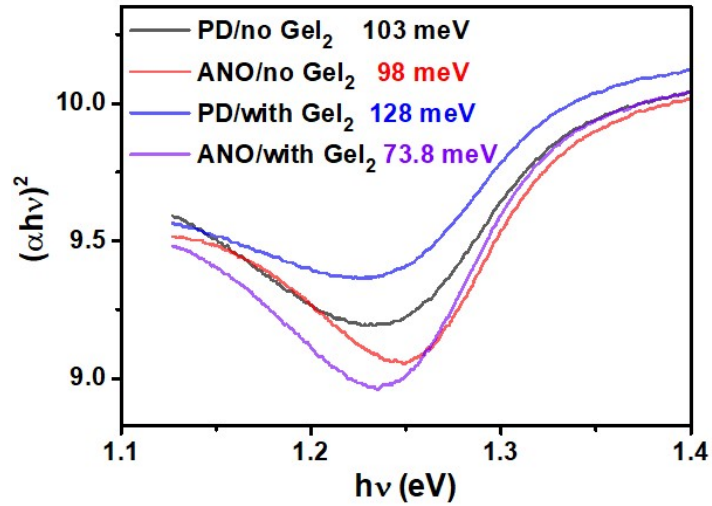


Fig. S12 Plots of $\ln(\alpha)$ versus $h\nu$ to extract the Urbach energy (E_u) of the Sn-Pb perovskite films. E_u can be determined using the relation $\alpha = \alpha_0 \exp(E/E_u)$, where α is the absorption coefficient and $E (= h\nu)$ is the photon energy.

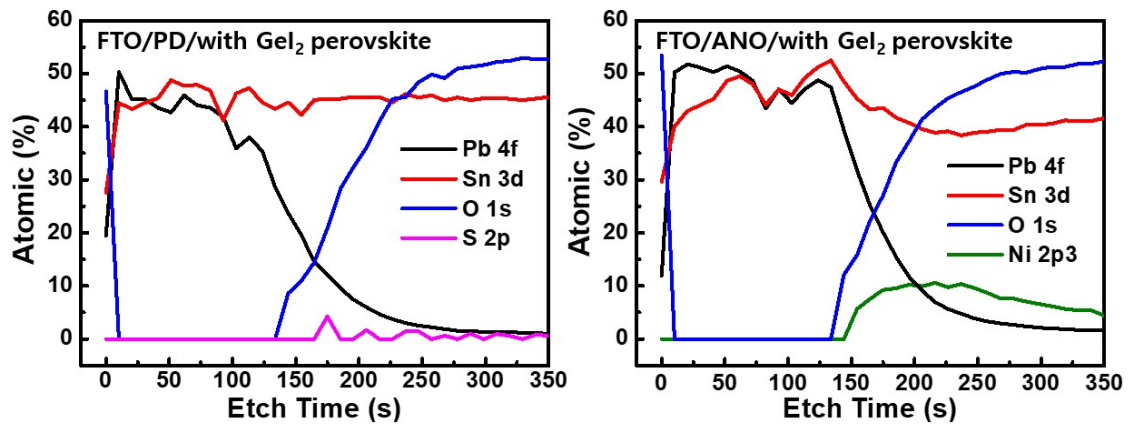


Fig. S13 The distribution of elements for FTO/PEDOT:PSS (PD) or ANO/with GeI_2 perovskite films.

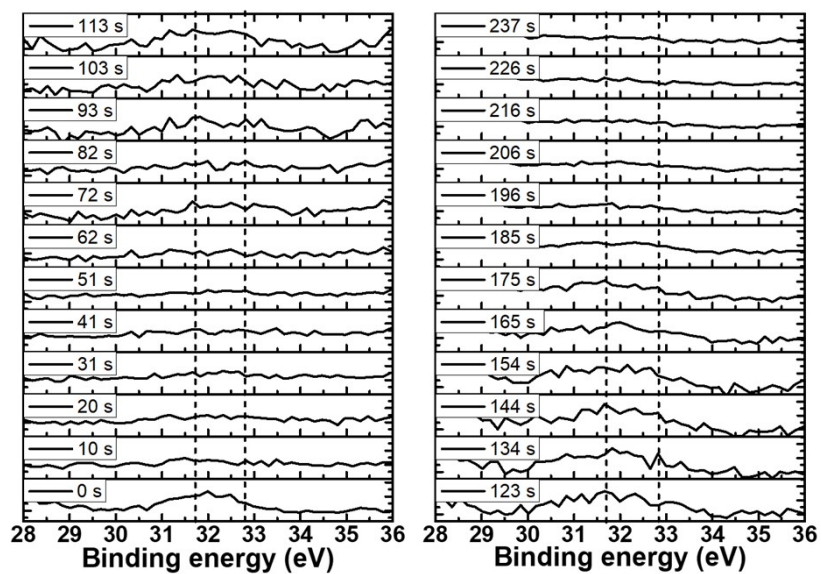


Fig. S14 Full XPS spectra of raw data for Ge 3d (GeO: 31.7 eV and GeO₂: 32.8 eV) of PD/with GeI₂ Sn-Pb perovskite film.

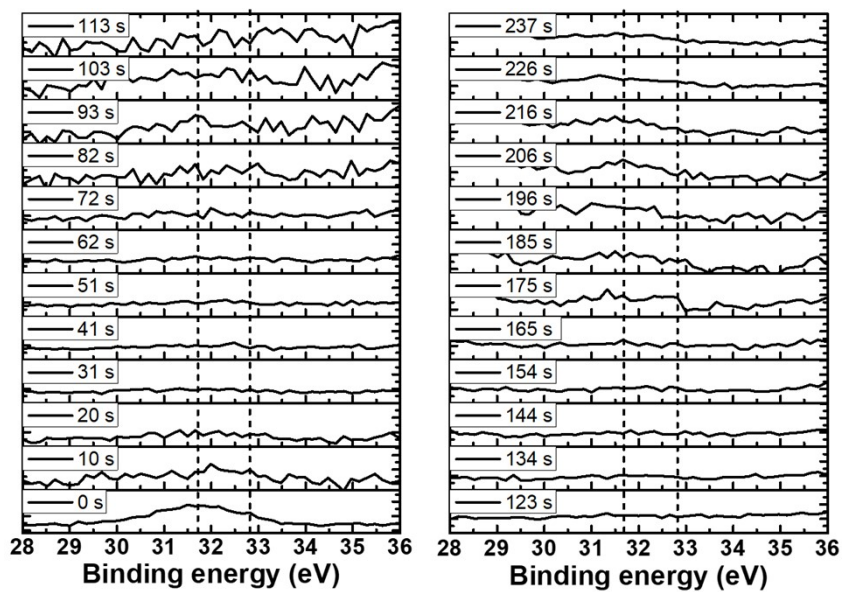


Fig. S15 Full XPS spectra of raw data for Ge 3d (GeO: 31.7 eV and GeO₂: 32.8 eV) of ANO/with GeI₂ Sn-Pb perovskite film.

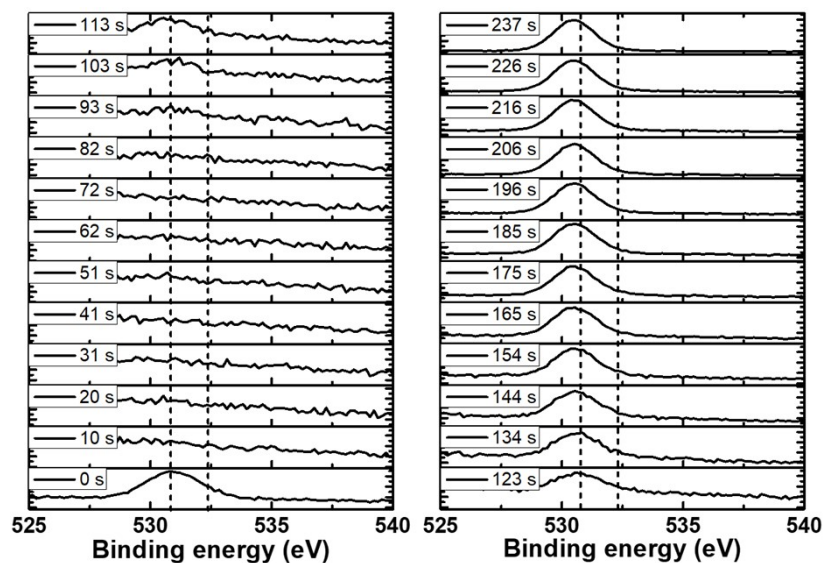


Fig. S16 Full XPS spectra of raw data for of O 1s (GeO: 530.8 eV and GeO₂: 532.4 eV) of PD/with GeI₂ Sn-Pb perovskite film.

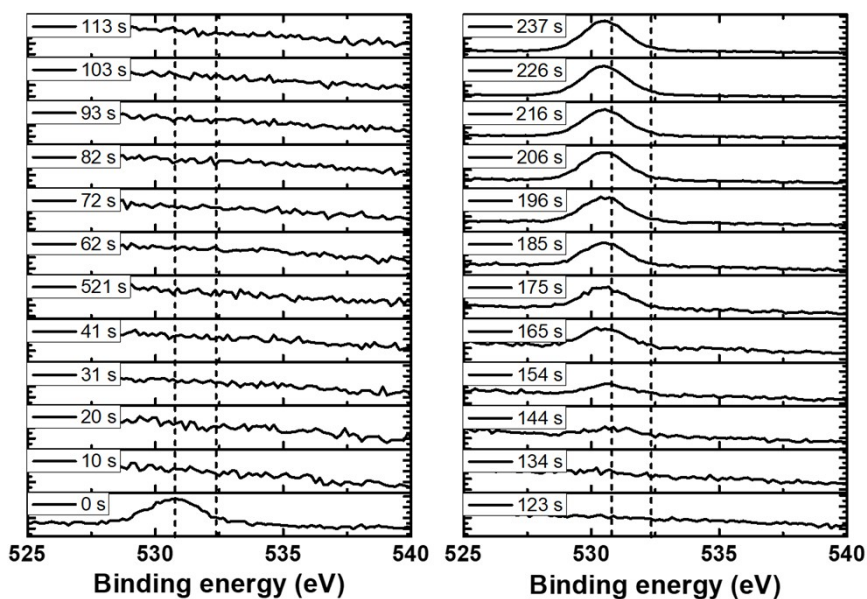


Fig. S17 Full XPS spectra of raw data for of O 1s (GeO: 530.8 eV and GeO₂: 532.4 eV) of ANO/with GeI₂ Sn-Pb perovskite film.

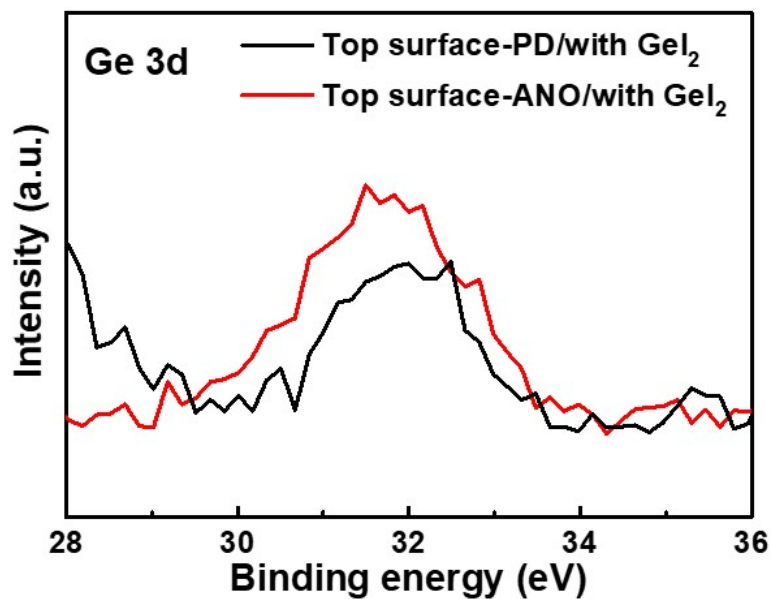


Fig. S18 Magnified Ge 3d XPS spectra for top surface of PD/with GeI₂ and ANO/with GeI₂ Sn-Pb perovskite films.

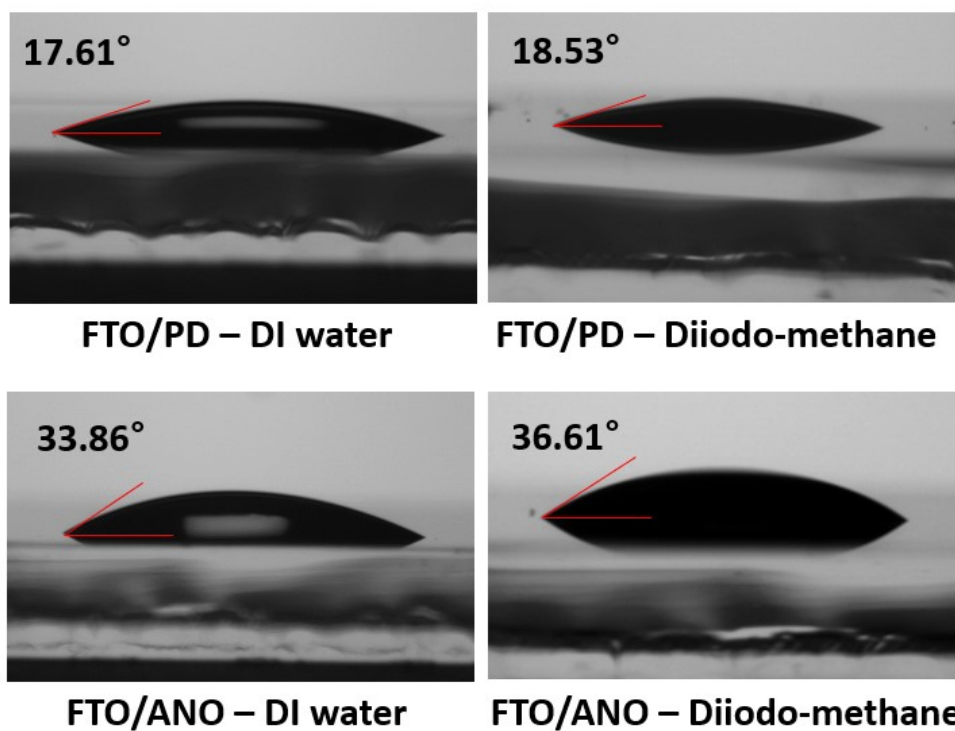


Fig. S19 Contact angles for PEDOT:PSS (PD) and ANO HTLs with DI water and diiodo-methane solvents.

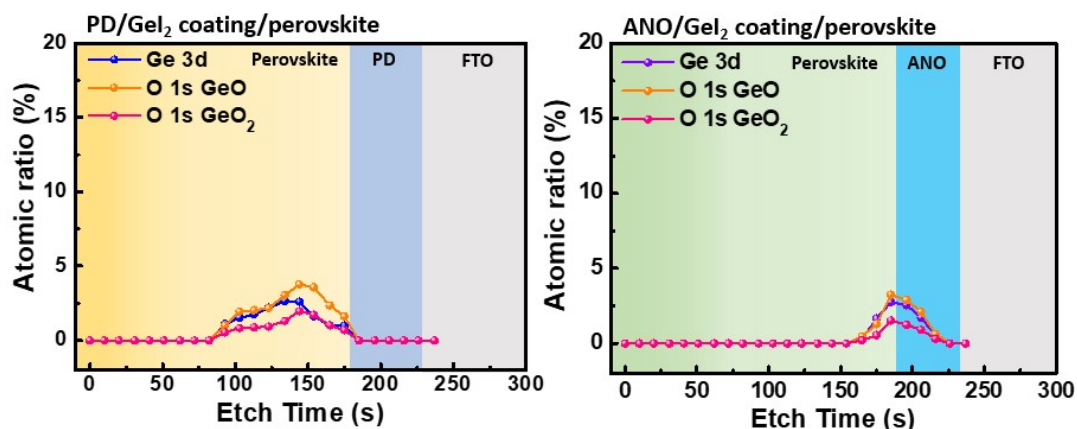


Fig. S20 Ge 3d and O 1s distribution for GeO_x of PEDOT:PSS (PD)/ GeI_2 coating/perovskite and ANO/ GeI_2 coating/perovskite films.

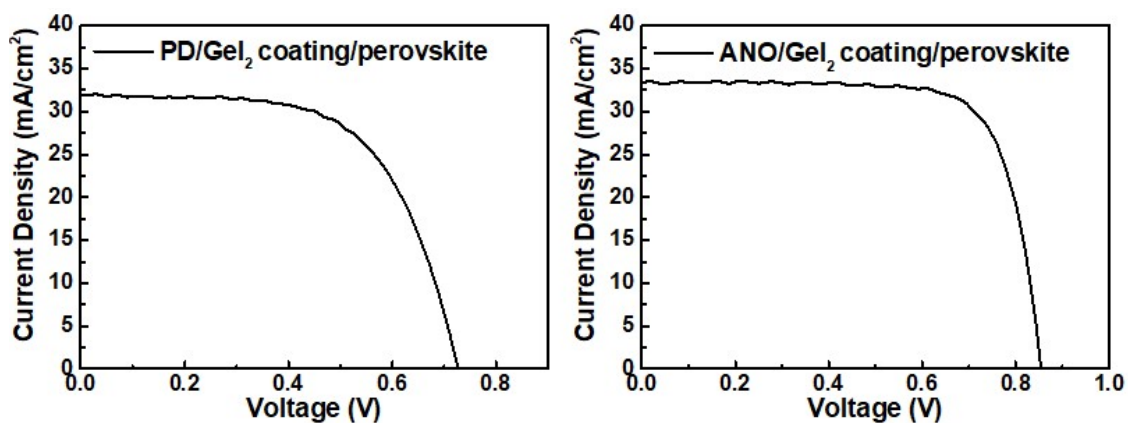


Fig. S21 Performance of the devices for PEDOT:PSS (PD)/ GeI_2 coating/perovskite and ANO/ GeI_2 (GeO_x) coating/perovskite conditions.

Table S5. Photovoltaic parameters of the devices for PD/ GeI_2 coating/perovskite and ANO/ GeI_2 coating/perovskite conditions

	V_{oc} (V)	J_{sc} (mA/cm ²)	FF (%)	PCE (%)
PD/ GeI_2 coating/perovskite	0.73	31.94	62.19	14.44
ANO/ GeI_2 coating/perovskite	0.86	33.33	75.48	21.52

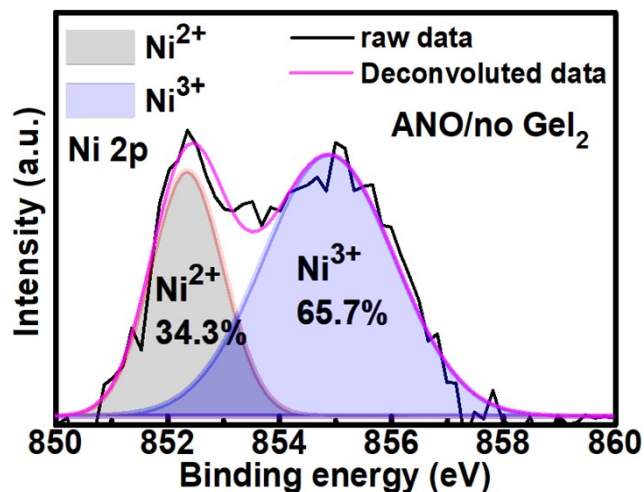


Fig. S22 Ni 2p XPS spectra of bottom surface for no GeI₂ Sn-Pb perovskite film on ANO.

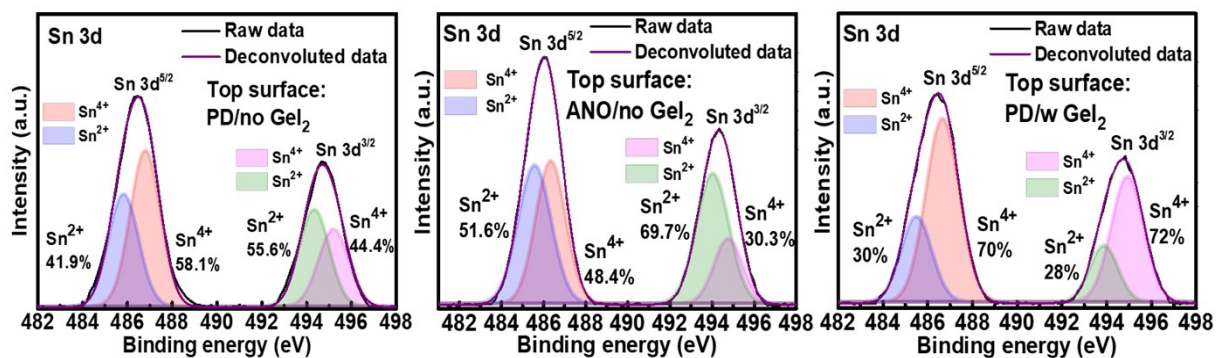


Fig. S23 Sn 3d XPS spectra for top surface of PD/no GeI₂, ANO/no GeI₂, and PD/with GeI₂ Sn-Pb perovskite films.

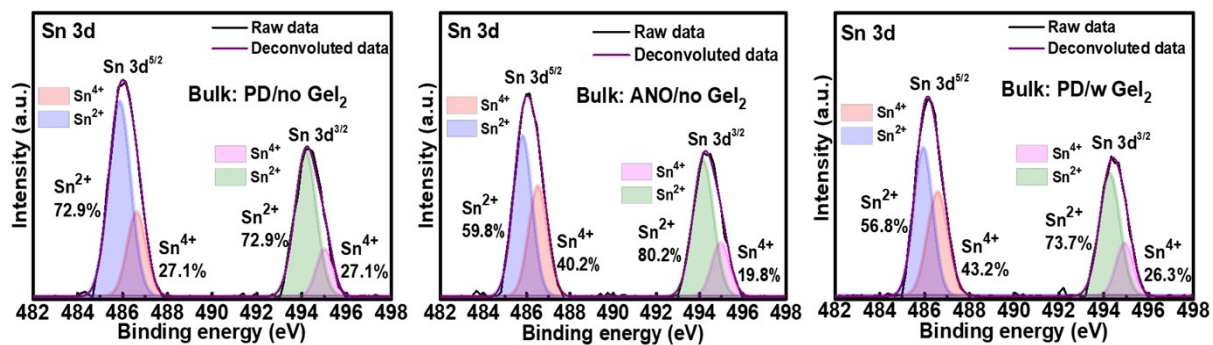


Fig. S24 Sn 3d XPS spectra for bulk of PD/no GeI₂, ANO/no GeI₂, and PD/with GeI₂ Sn-Pb perovskite films.

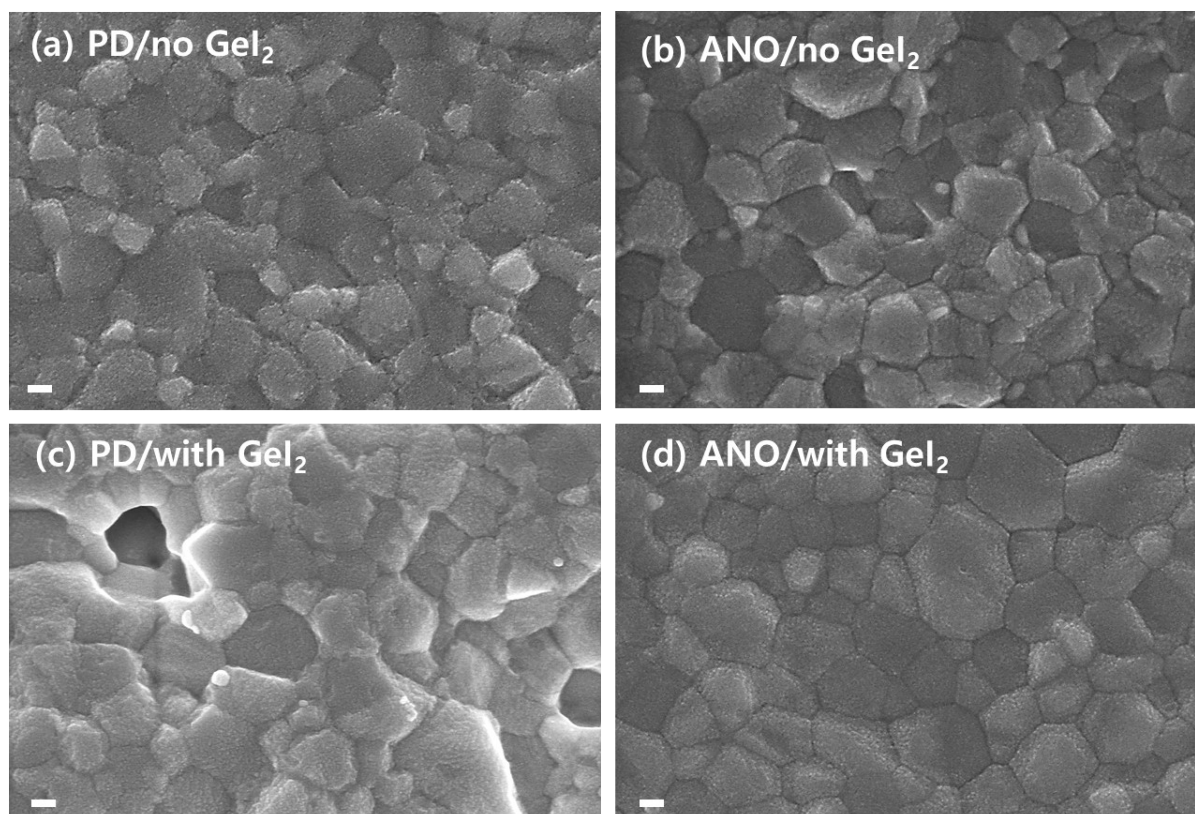


Fig. S25 FE-SEM morphology images of perovskite films of (a) PD/no GeI₂, (b) ANO/no GeI₂, (c) PD/with GeI₂, and (d) ANO/with GeI₂. Scale bar: 100 nm.

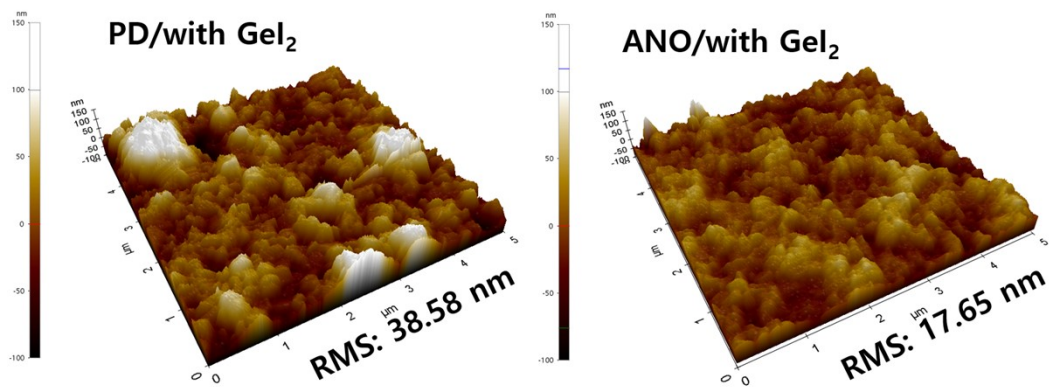


Fig. S26 AFM 3D images showing the surface roughness of PD/with GeI_2 and ANO/with GeI_2 films.

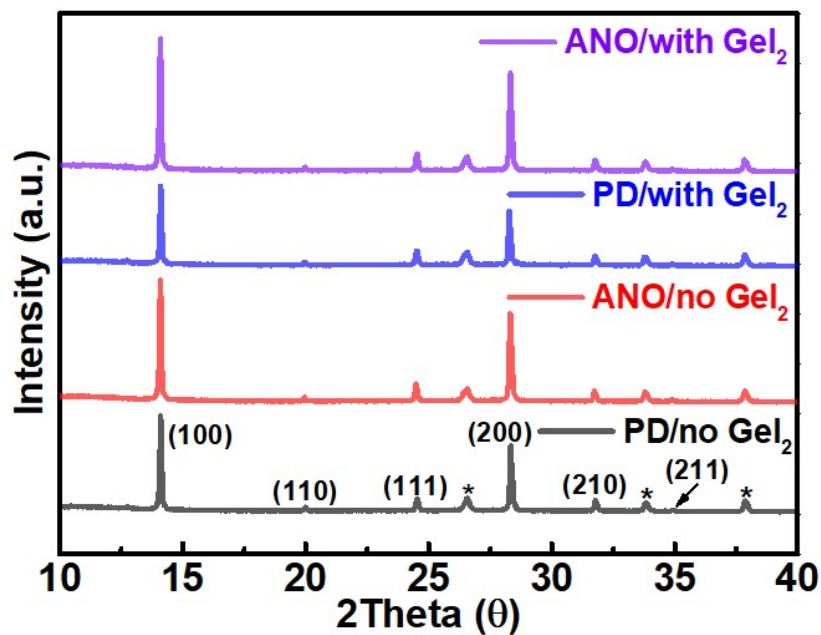


Fig. S27 XRD patterns for the Sn-Pb perovskite films with suggested conditions (PD/no GeI_2 , ANO/no GeI_2 , PD/with GeI_2 , and ANO/with GeI_2). * Marks are FTO peaks.

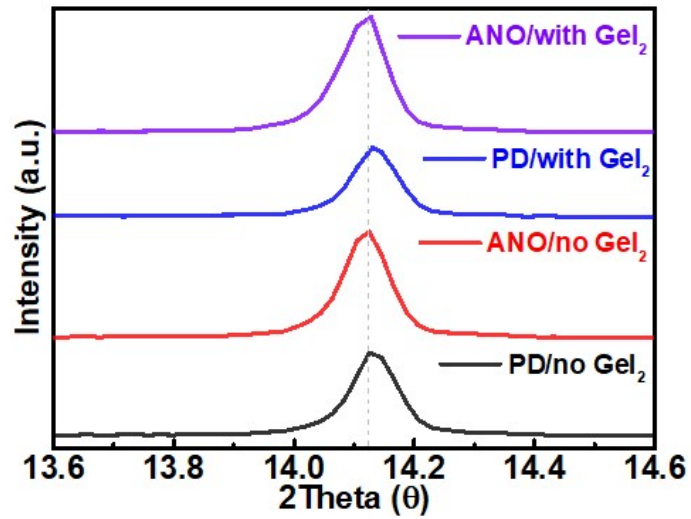


Fig. S28 The magnified XRD patterns for main perovskite peaks of PD/no GeI_2 , ANO/no GeI_2 , PD/with GeI_2 and ANO/with GeI_2 .

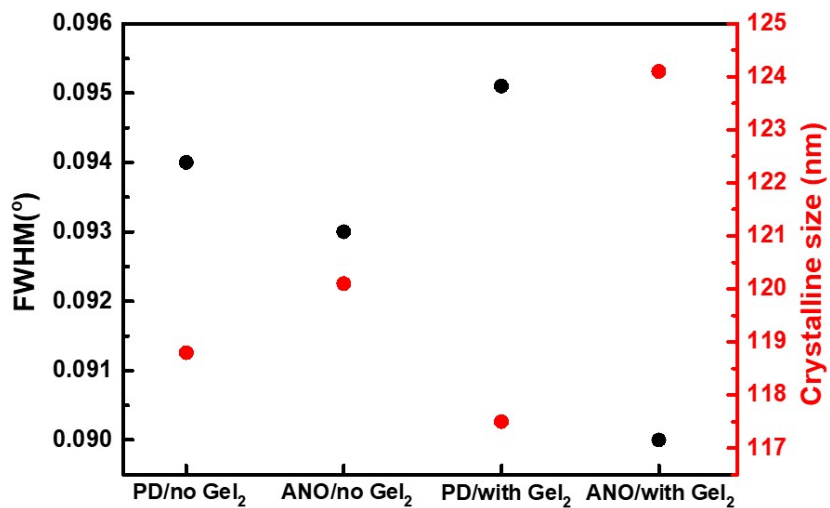


Fig. S29 FWHM values (left axis) and calculated crystalline sizes (right axis) from the (100) lattice plane.

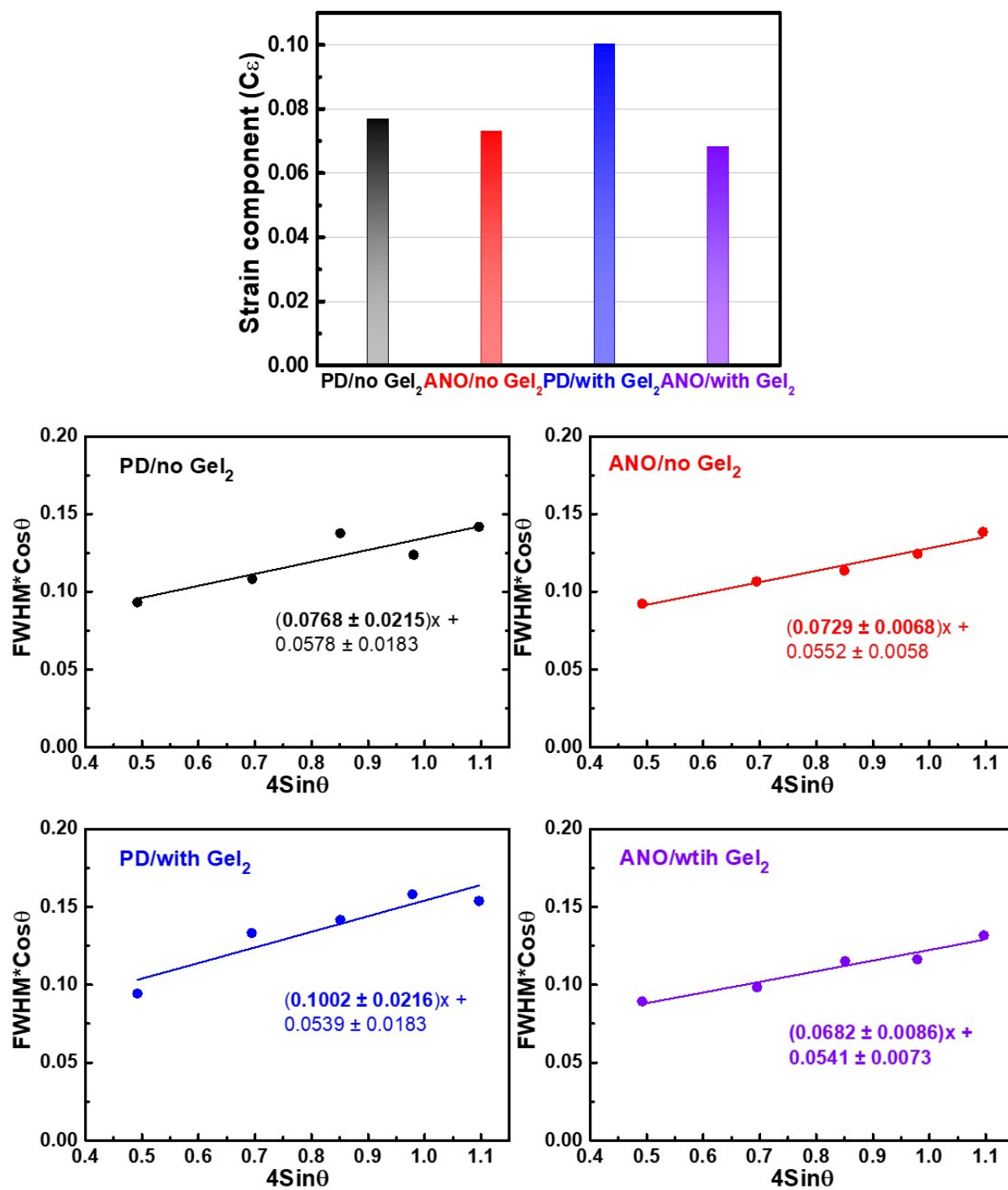


Fig. S30 Change of strain component (C_ϵ) of perovskite films fabricated on different HTLs (PD and ANO) and without or with GeI_2 additive. Williamson-Hall plots to determine the strain component (C_ϵ) in the Sn-Pb perovskite films with PD/no GeI_2 , ANO/no GeI_2 , PD/with GeI_2 , and ANO/with GeI_2 conditions.

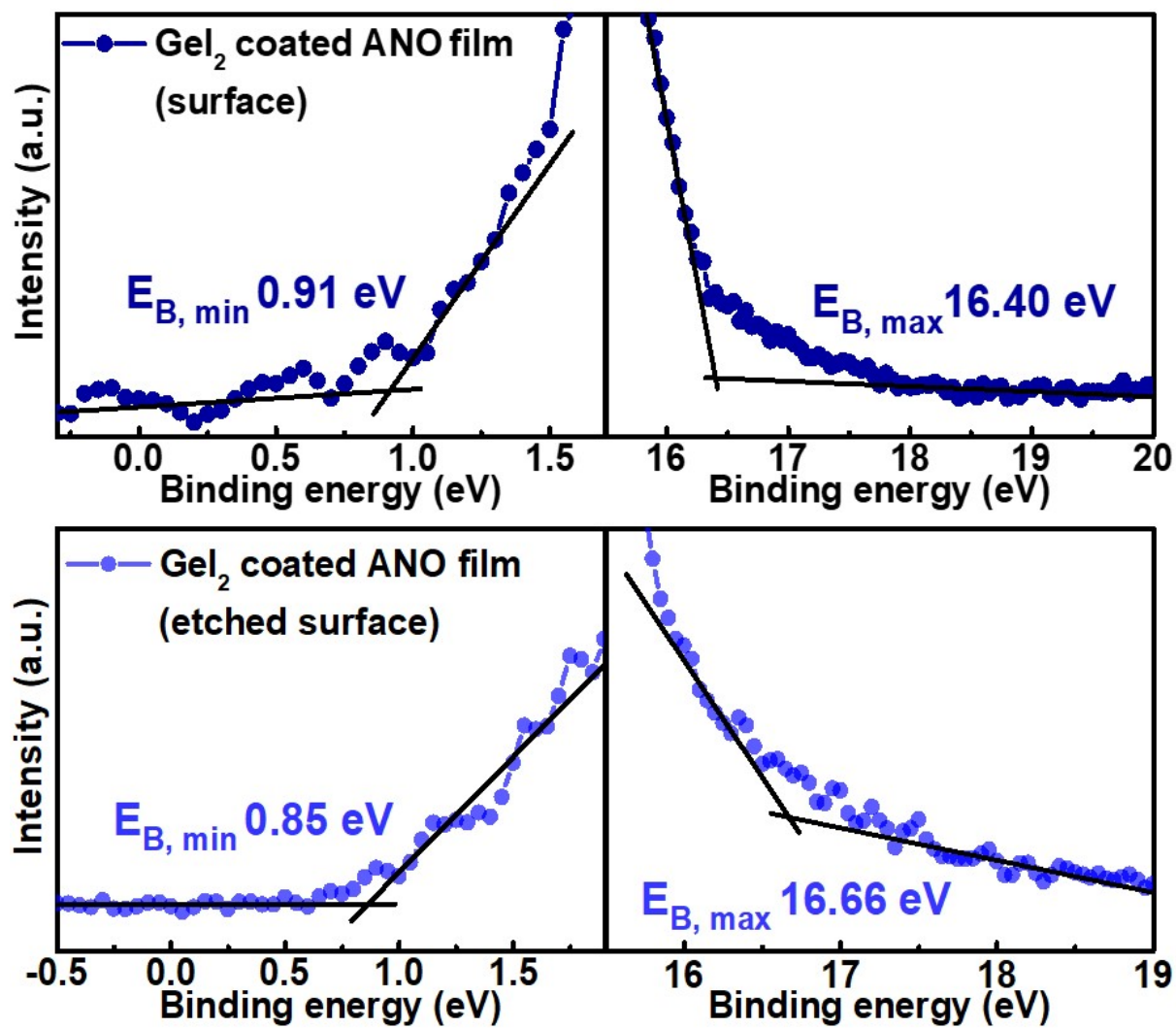


Fig. S31 UPS spectra of secondary electron cutoff and valence band of GeI_2 -coated ANO films without etching and with etching.

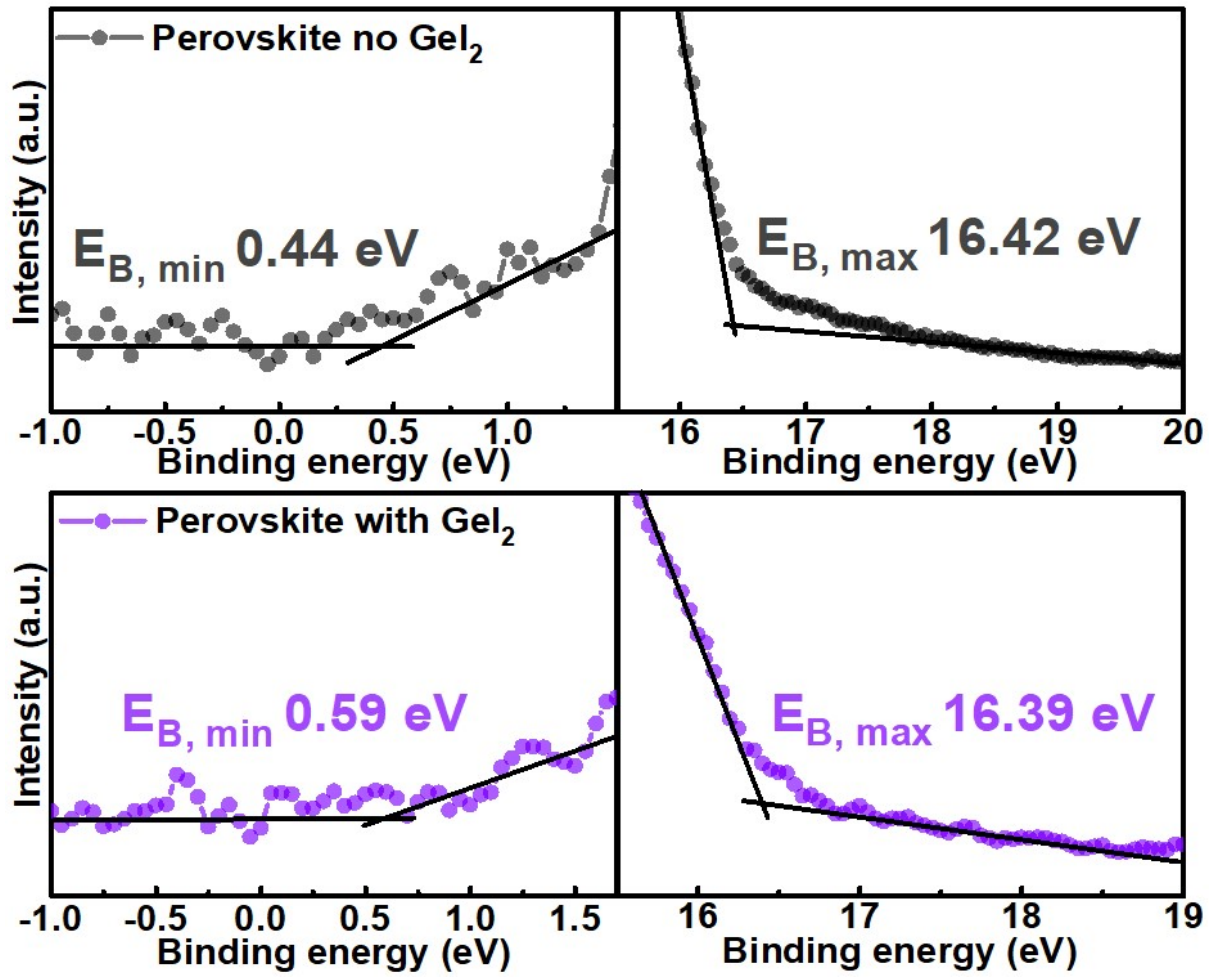


Fig. S32 UPS spectra of secondary electron cutoff and valence band of control no GeI₂ perovskite and with GeI₂ perovskite films.

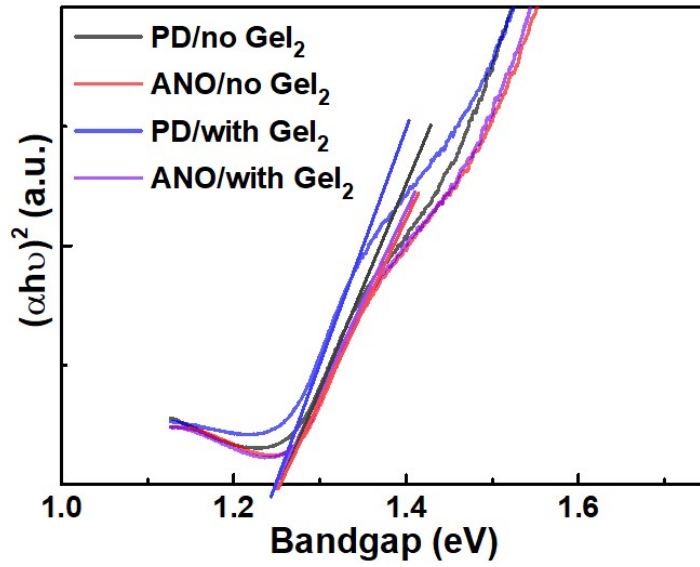


Fig. S33 Tauc plots of the perovskite films with PD/no GeI_2 , ANO/no GeI_2 , PD/with GeI_2 , and ANO/with GeI_2 conditions. The bandgap of MA-free Sn-Pb perovskite is 1.25 eV.

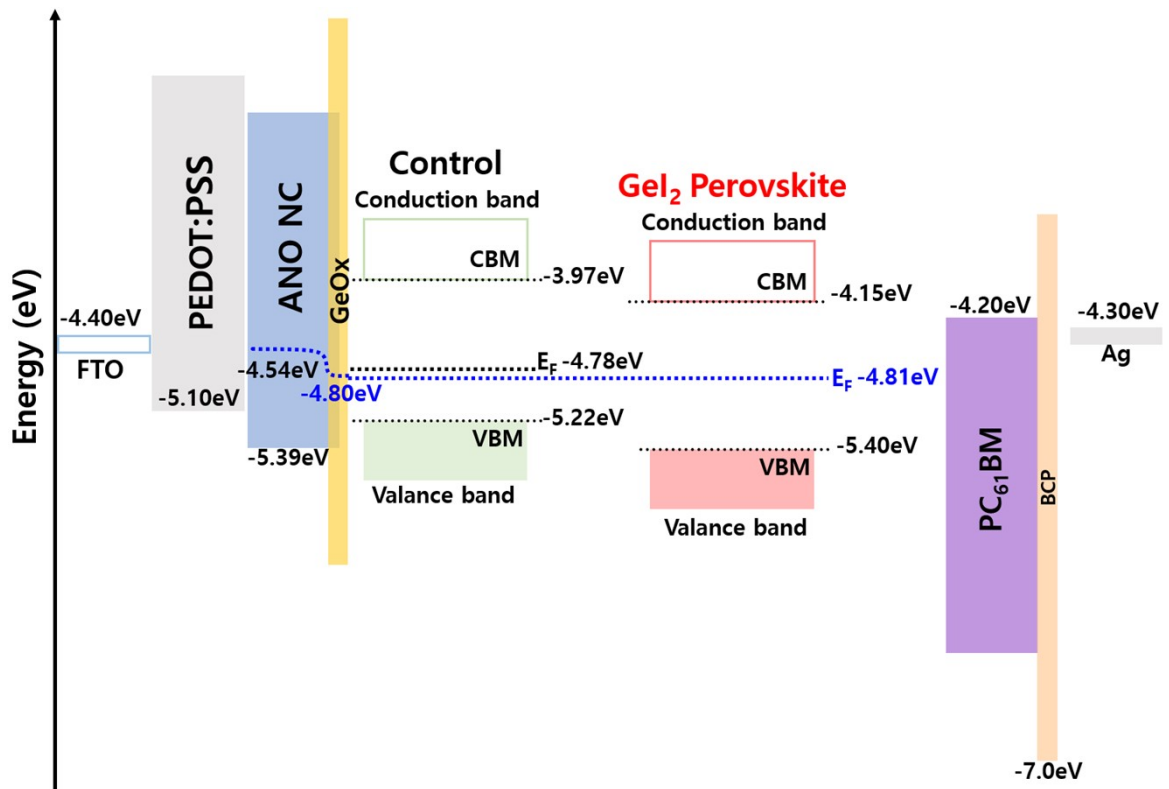


Fig. S34 Energy band diagram of the fabricated MA-free Sn-Pb PSCs.

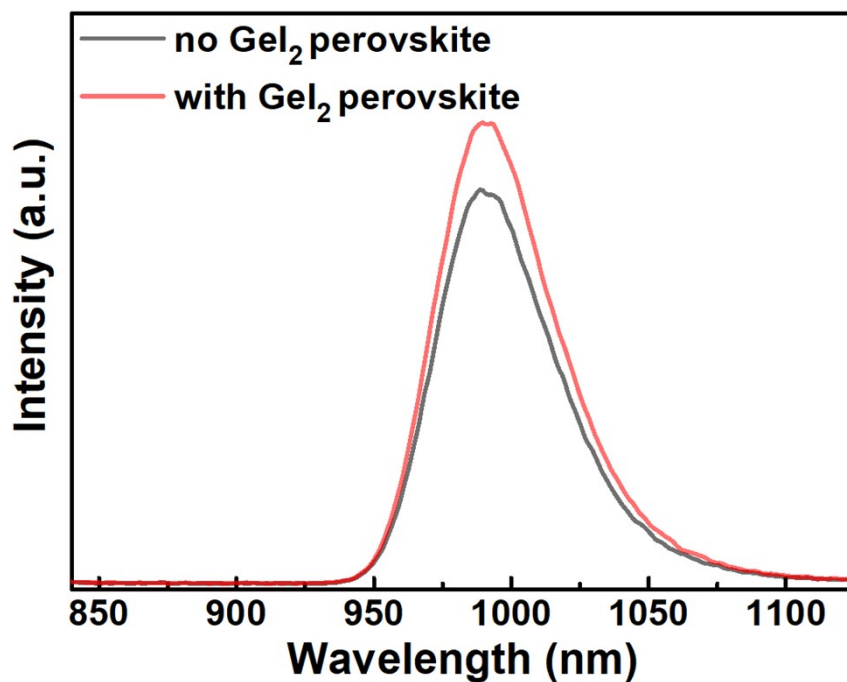


Fig. S35 Steady-state photoluminescence (SS-PL) spectra of bare glass/perovskite films of no GeI_2 and with GeI_2 conditions.

Table S6. TR-PL decay obtained after fitting for bare glass/perovskite films with no GeI_2 and with GeI_2 shown in Fig. S35.

	τ_1 (ns)	τ_2 (ns)	τ_{avg} (ns)
no GeI_2	136.31	605.89	341.18
with GeI_2	147.87	764.92	482.13

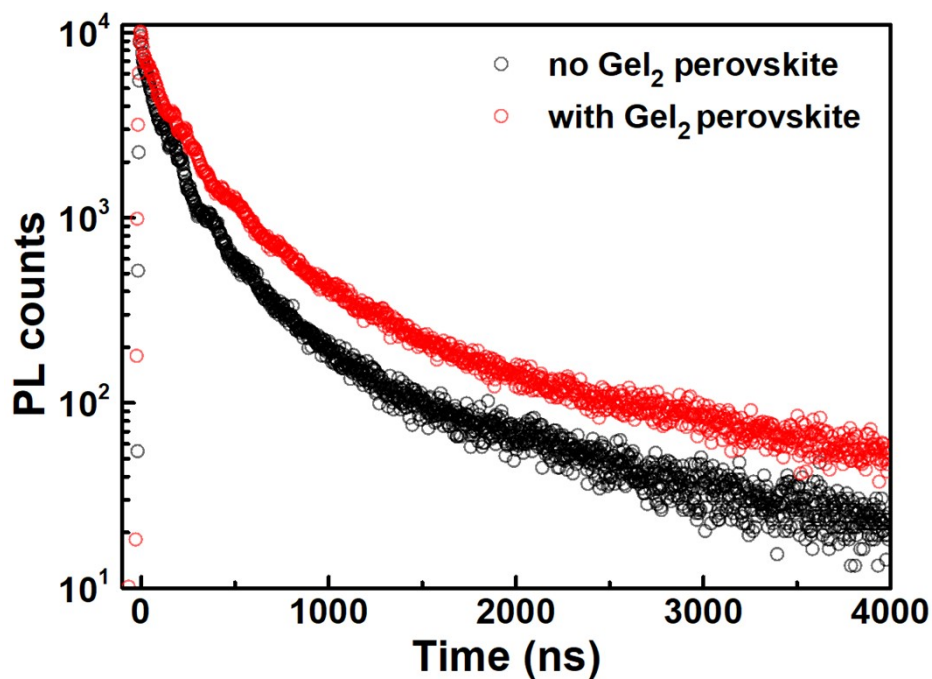


Fig. S36 Time-resolved photoluminescence (TR-PL) spectra of bare glass/perovskite films with no GeI₂ and with GeI₂.

Table S7. TR-PL decay obtained after fitting for PD/no GeI₂, ANO/no GeI₂, PD/with GeI₂, and ANO/with GeI₂ perovskite films shown in Fig. S36.

	τ_1 (ns)	τ_2 (ns)	τ_{avg} (ns)
PD/no GeI ₂	14.06	344.91	39.04
ANO/no GeI ₂	17.92	424.18	51.37
PD/with GeI ₂	38.41	326.34	115.01
ANO/with GeI ₂	10.23	346.80	16.32

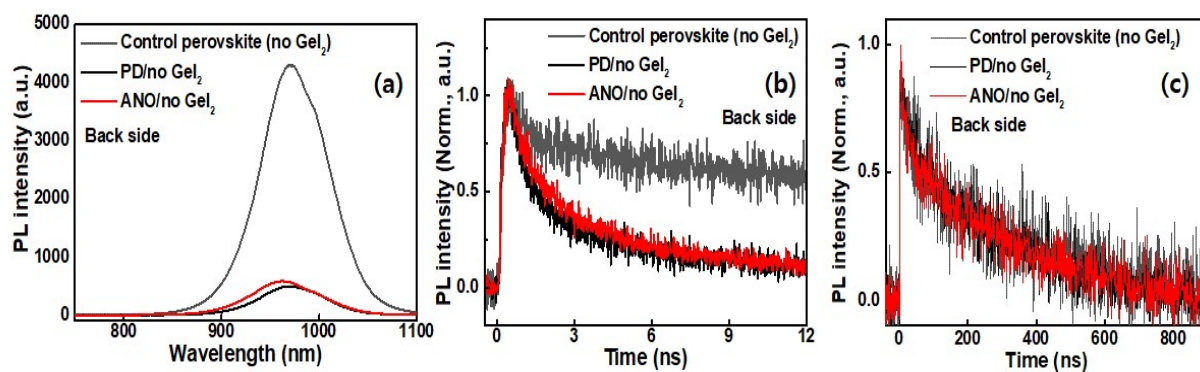


Fig. S37 PL analysis for back side (glass side) of glass/PEDOT:PSS (PD) or ANO/control perovskite no GeI_2 (a) SS-PL spectra of glass/control perovskite no GeI_2 , glass/PD/control perovskite no GeI_2 and glass/ANO/control perovskite no GeI_2 . (b) TR-PL spectra of glass/control perovskite no GeI_2 , glass/PD/control perovskite no GeI_2 and glass/ANO/control perovskite no GeI_2 with 12 ns time window. (c) TR-PL spectra of glass/control perovskite no GeI_2 , glass/PD/control perovskite no GeI_2 and glass/ANO/control perovskite no GeI_2 with 1000 ns time window.

Table S8. TR-PL decay obtained after fitting for back side of glass/PD or ANO/no GeI_2 perovskite films with 12 ns and 1000 ns time windows in Fig. S37

	Fitted time constants (ns)		
	τ_1	τ_2	τ_3
Control perovskite (no GeI_2)	3.0 (40%)	400 (60%)	
PD/no GeI_2	1.7 (59%)	3.0 (34%)	400 (7%)
ANO/no GeI_2	2.1 (47%)	3.5 (44%)	400 (9%)

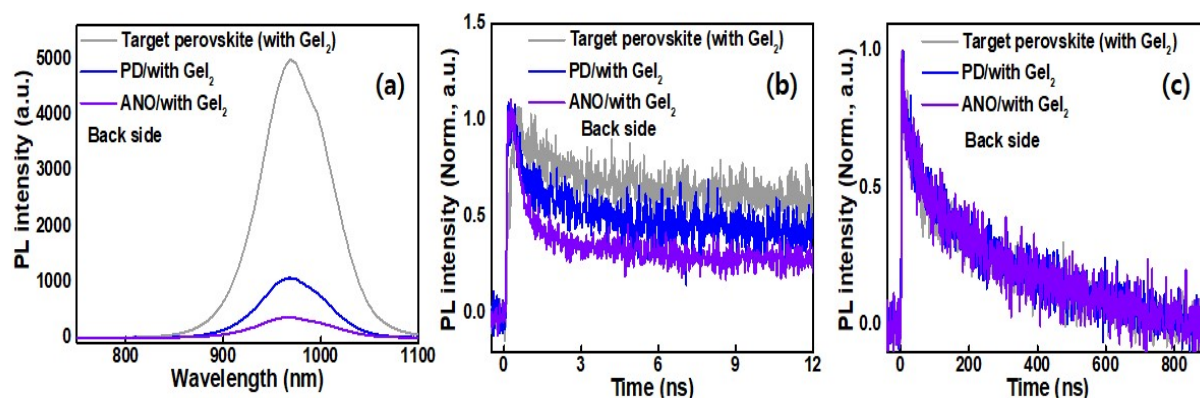


Fig. S38 PL analysis for back side (glass side) of glass/PEDOT:PSS (PD) or ANO/target perovskite with GeI_2 (a) SS-PL spectra of glass/target perovskite with GeI_2 , glass/PD/target perovskite with GeI_2 and glass/ANO/target perovskite with GeI_2 . (b) TR-PL spectra of glass/target perovskite with GeI_2 , glass/PD/target perovskite with GeI_2 and glass/ANO/target perovskite with GeI_2 with 12 ns time window. (c) TR-PL spectra of glass/target perovskite with GeI_2 , glass/PD/target perovskite with GeI_2 and glass/ANO/target perovskite with GeI_2 with 1000 ns time window.

Table S9. TR-PL decay obtained after fitting for back side of glass/PD or ANO/with GeI_2 perovskite films with 12 ns and 1000 ns time windows in Fig. S38

	Fitted time constants (ns)		
	τ_1	τ_2	τ_3
Target perovskite (with GeI_2)	4.0 (37%)	400 (63%)	
PD/with GeI_2	1.4 (52%)	4.0 (10%)	400 (38%)
ANO/with GeI_2	1.2 (76%)	400 (24%)	

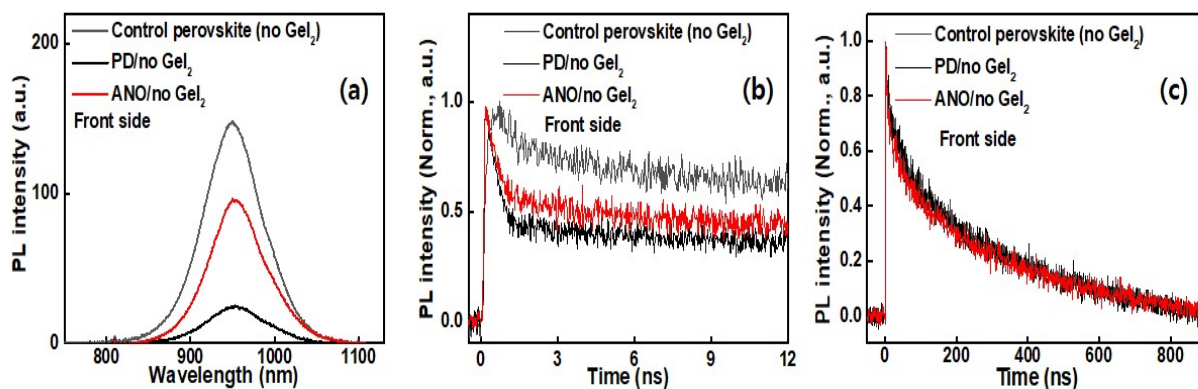


Fig. S39 PL analysis for front side (perovskite side) of glass/PEDOT:PSS (PD) or ANO/control perovskite no GeI_2 (a) SS-PL spectra of glass/control perovskite no GeI_2 , glass/PD/control perovskite no GeI_2 and glass/ANO/control perovskite no GeI_2 . (b) TR-PL spectra of glass/ANO/control perovskite no GeI_2 , glass/PD/control perovskite no GeI_2 and glass/ANO/control perovskite no GeI_2 with 12 ns time window. (c) TR-PL spectra of glass/control perovskite no GeI_2 , glass/PD/control perovskite no GeI_2 and glass/ANO/control perovskite no GeI_2 with 1000 ns time window.

Table S10. TR-PL decay obtained after fitting for front side of glass/PD or ANO/no GeI_2 perovskite films with 12 ns and 1000 ns time windows in Fig. S39

	Fitted decay times (ns)		
	τ_1	τ_2	τ_3
Control perovskite (no GeI_2)	3.0 (37%)	400 (63%)	
PD/no GeI_2	0.9 (70%)	3.0 (4%)	400 (26%)
ANO/no GeI_2	1.2 (64%)	3.5 (11%)	400 (25%)

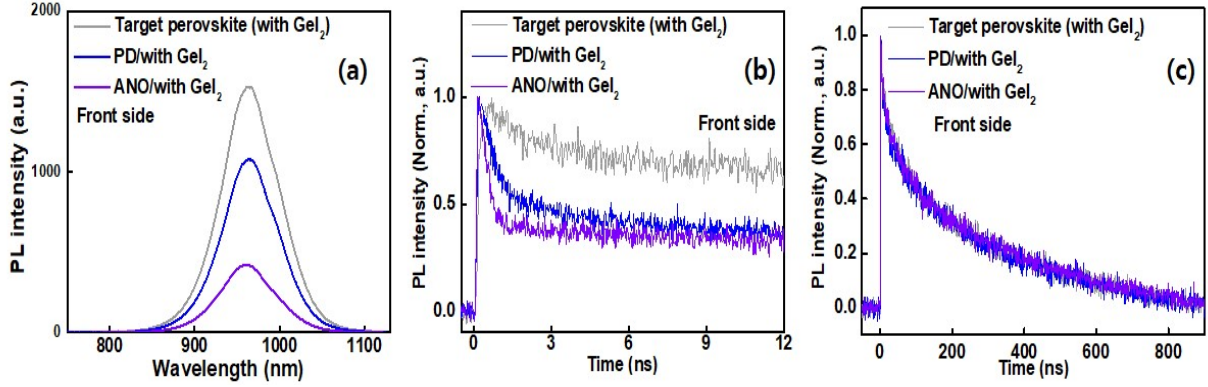


Fig. S40 PL analysis for front side (perovskite side) of glass/PEDOT:PSS (PD) or ANO/target perovskite with GeI_2 (a) SS-PL spectra of glass/target perovskite with GeI_2 , glass/PD/target perovskite with GeI_2 and glass/ANO/target perovskite with GeI_2 . (b) TR-PL spectra of glass/target perovskite with GeI_2 , glass/PD/target perovskite with GeI_2 and glass/ANO/target perovskite with GeI_2 with 12 ns time window. (c) TR-PL spectra of glass/target perovskite with GeI_2 , glass/PD/target perovskite with GeI_2 and glass/ANO/target perovskite with GeI_2 with 1000 ns time window.

Table S11. TR-PL decay obtained after fitting for front side of glass/PD or ANO/with GeI_2 perovskite films with 12 ns and 1000 ns time windows in Fig. S40

	Fitted decay times (ns)		
	τ_1	τ_2	τ_3
Target perovskite (with GeI_2)	4.0 (34%)	400 (66%)	
PD/with GeI_2	1.5 (60%)	4.0 (10%)	400 (30%)
ANO/with GeI_2	0.8 (73%)	4.0 (5%)	400 (22%)

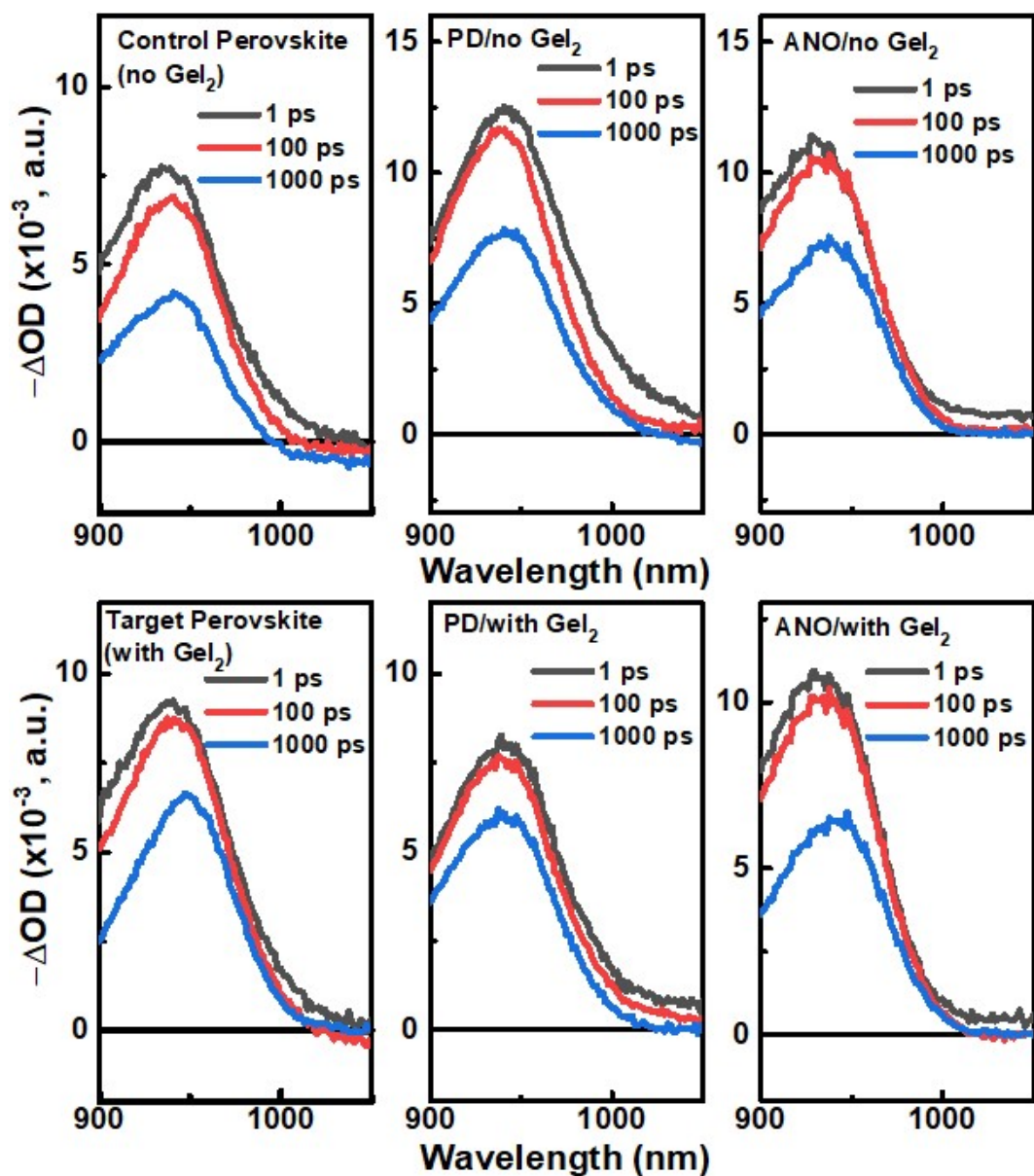


Fig. S41 Femtosecond-TAS spectra ΔOD as a function of wavelength at selected delay times using a photoexcitation wavelength of 400 nm and a pump fluence of $3 \mu\text{J}/\text{cm}^2$.

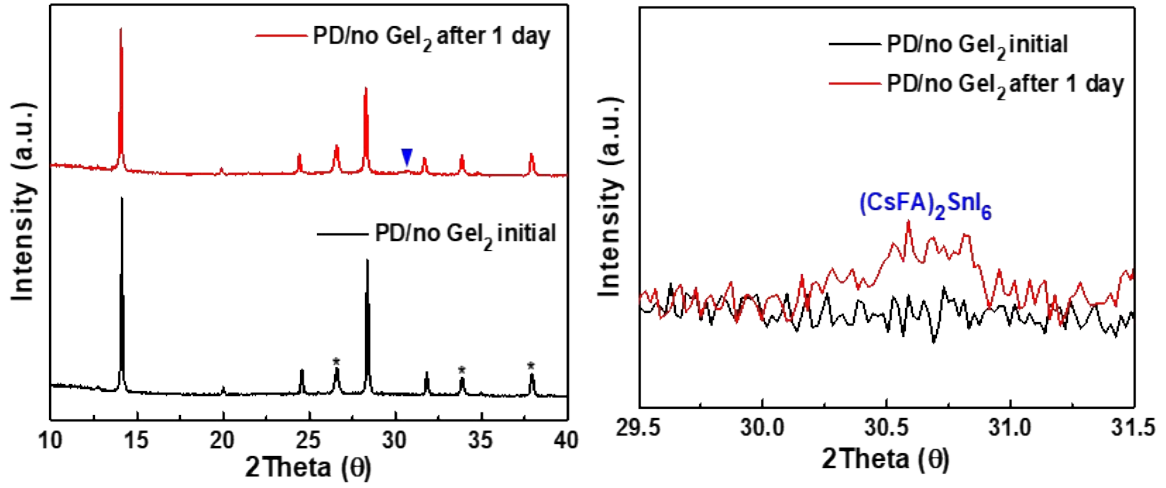


Fig. S42. Time-dependent XRD patterns of PD/no GeI₂ perovskite film.

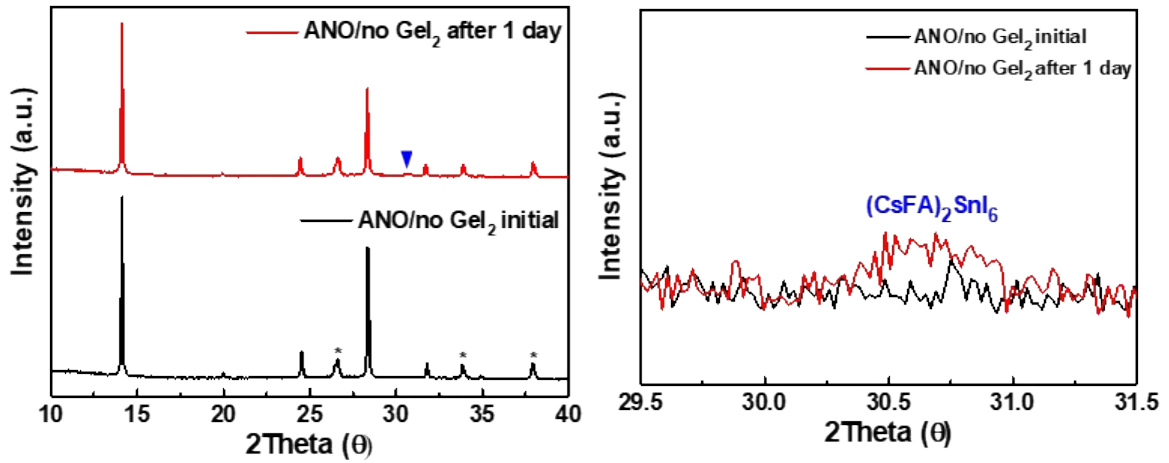


Fig. S43. Time-dependent XRD patterns of ANO/no GeI₂ perovskite film.

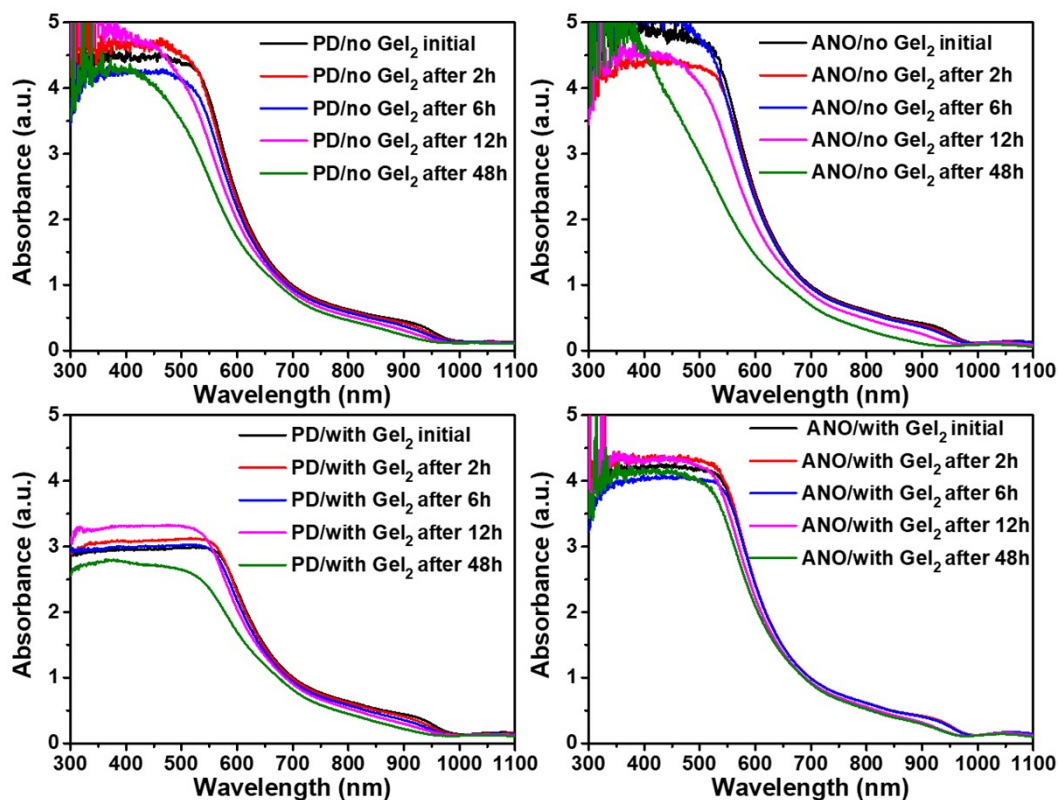


Fig. S44. Time-dependent absorption spectra of PD/no GeI₂, ANO/no GeI₂, PD/with GeI₂, and ANO/with GeI₂ fabricated on FTO.

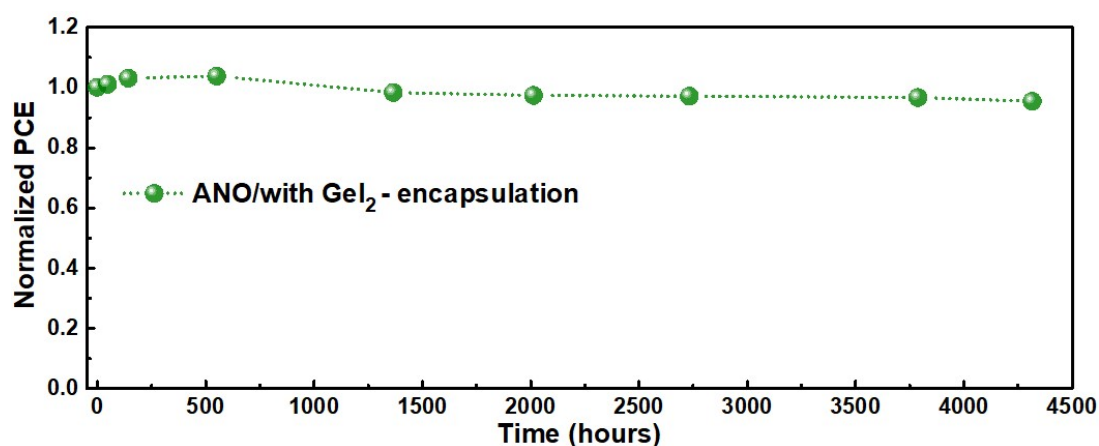


Fig. S45. Long-term stability of the MA-free Sn-Pb PSCs of ANO/with GeI₂ condition with encapsulation.

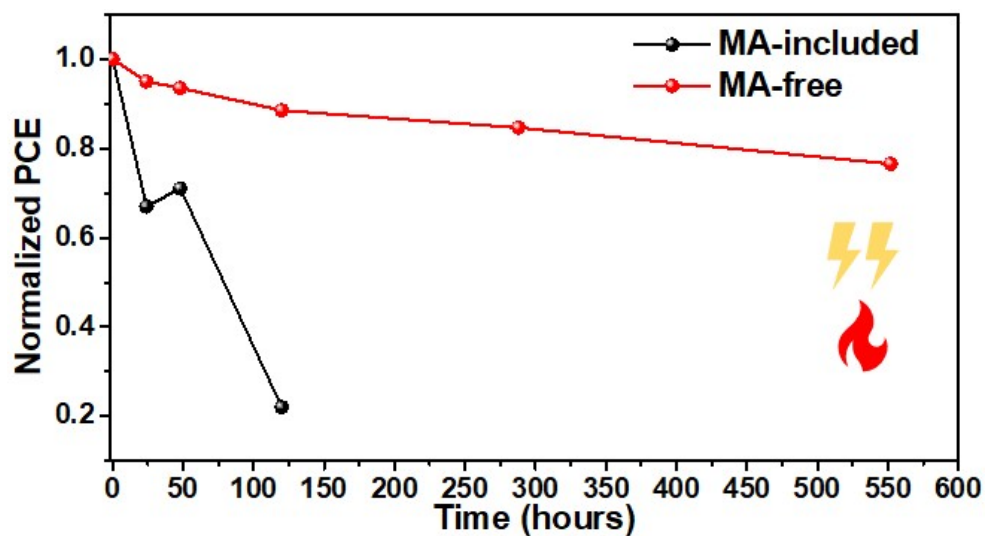


Fig. S46 The normalized light-thermal stability of the MA-included and MA-free Sn-Pb perovskite solar cells under 55 °C and 100 mW/cm² illumination of LED simulator.

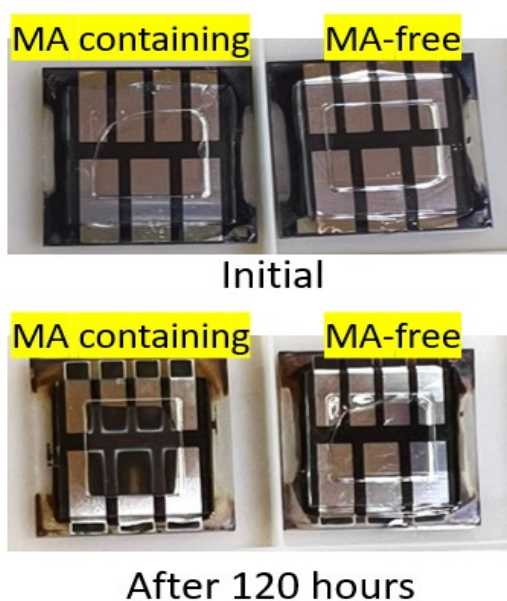


Fig. S47 Photographs of MA-containing Sn-Pb PSC and MA-free Sn-Pb PSC with initial and after 120 hours

References

1. S. Shao, Y. Cui, H. Duim, X. Qiu, J. Dong, G. H. Ten Brink, G. Portale, R. C. Chiechi, S. Zhang, J. Hou and M. A. Loi, *Adv. Mater.*, 2018, **30**, 1803703.
2. D. Chi, S. Huang, M. Zhang, S. Mu, Y. Zhao, Y. Chen and J. You, *Adv. Funct. Mater.*, 2018, **28**, 1804603.
3. J. Werner, T. Moot, T. A. Gossett, I. E. Gould, A. F. Palmstrom, E. J. Wolf, C. C. Boyd, M. F. van Hest, J. M. Luther, J. J. Berry and M. D. McGehee, *ACS Energy Lett.*, 2020, **5**, 1215-1223.
4. W. Zhang, X. Li, S. Fu, X. Zhao, X. Feng and J. Fang, *Joule*, 2021, **5**, 2904-2914.
5. H. Guo, H. Zhang, S. Liu, D. Zhang, Y. Wu and W.-H. Zhu, *ACS Appl. Mater. Interfaces*, 2022, **14**, 6852-6858.
6. Z. Yu, J. Wang, B. Chen, M. A. Uddin, Z. Ni, G. Yang and J. Huang, *Adv. Mater.*, 2022, **34**, 2205769.
7. J. Wang, Z. Yu, D. D. Astridge, Z. Ni, L. Zhao, B. Chen, M. Wang, Y. Zhou, G. Yang, X. Dai, A. Sellinger and J. Huang, *ACS Energy Lett.*, 2022, **7**, 3353-3361.
8. M. Pitaro, J. E. S. Alonso, L. Di Mario, D. G. Romero, K. Tran, J. Kardula, T. Zaharia, M. B. Johansson, E. M. Johansson, R. C. Chiechi and M. A. Loi, *Adv. Funct. Mater.*, 2023, 2306571.
9. M. Pitaro, J. S. Alonso, L. Di Mario, D. G. Romero, K. Tran, T. Zaharia, M. B. Johansson, E. M. Johansson and M. A. Loi, *J. Mater. Chem. A*, 2023, **11**, 11755-11766.
10. Y. Zhou, Z. Wang, J. Jin, X. Zhang, J. Zou, F. Yao, Z. Zhu, X. Cui, D. Zhang, Y. Yu, C. Chen, D. Zhao, Q. Cao, Q. Lin and Q. Tai, *Angew. Chem. Int. Edit.*, 2023, **135**, e202300759.